Sl. No.	IIT Ropar List of Recent Publications with Abstract Coverage: February, 2025
A	**Book Chapter(s)**
1.	Constrained path optimization on time-dependent road networks **KK Dutta, VMV Gunturi** - Web Information Systems Engineering – WISE 2024 PhD Symposium, Demos and Workshops, Book Chapter, 2025 **Abstract:** Time-Dependent Constrained Path Optimization (TD-CPO) takes the following input: (i) time-dependent (TD) road network, (ii) source (*s*), (iii) destination (*d*), (iv) departure time (*t*) and, (v) budget (B). In a TD road network, each edge is characterized by a time-dependent arrival time and a score function. TD-CPO aims to determine a loopless *s*–*d* path which departs from *s* at time *t* and arrives at *d* on or before time t+B while maximizing the score. TD-CPO has applications in urban navigation. TD-CPO is a variant of the Arc Orienteering Problem (AOP) known to be NP-hard in nature The key computational challenge of TD-CPO is that we need to find the "longest path" in terms of score within the given budget constraint in a TD road network. Current algorithms either prune down search space aggressively, leading to low solution quality or are not scalable to large networks. In contrast, our proposed approach SCOPE explores a comprehensive search space efficiently. Furthermore, the inherent computational structure of SCOPE enables trivial parallelization for improved performance. Our experiments indicate that SCOPE achieves both superior quality solutions (nearly 2X) and acceptable runtimes (within 3 secs) when compared to the state-of-the-art algorithm on large road networks. Furthermore, SCOPE exhibits almost linear speedup as the number of CPU cores increases.
2.	Hydrogen storage and transportation: Utilizing liquid organic hydrogen carriers and existing natural gas pipelines **Y Saini, A Singh, DK Mahajan, H Tyagi** - Adaptive Engineering: A Sustainable Development Endeavor, Book Chapter, 2025 **Abstract:** Global efforts are increasingly focused on addressing the detrimental impacts of pollution resulting from human activities and leading to environmental degradation, including global warming, climate change, and ozone layer depletion. Energy generation is a significant contributor to pollution, emphasizing the need for cleaner alternatives. While renewable energy sources such as wind, solar, and hydropower show promise for stationary power generation, electric vehicles are emerging as a solution for mobile applications. However, challenges persist in terms of widespread charging infrastructure. Hydrogen energy, a clean and transportable energy carrier, is gaining prominence as a solution. The primary hindrance to the widespread use of hydrogen as an energy source lies in its storage and transportation. This issue stems from hydrogen's low volumetric energy density in its gaseous state, making traditional methods economically unviable. To overcome this challenge, the concept of liquid organic hydrogen carriers (LOHCs) has emerged. LOHCs involve chemically bonding hydrogen to organic compounds, such as toluene, rendering hydrogen safe for handling and transport. When needed, the LOHC undergoes a dehydrogenation reaction to release hydrogen, along with the original organic compound, which can be recycled. However, the LOHC method has its challenges, including high round-trip costs associated with transporting the LOHC back for hydrogenation after dehydrogenation and the gradual deterioration of LOHC quality over multiple cycles. These issues necessitate ongoing research and development efforts to enhance economic viability. One promising solution to address the economic challenges of LOHC transportation is the repurposing of existing natural gas pipelines. By reconfiguring these pipelines for LOHC transport and strategically placing hydrogenation and dehydrogenation units at locations where

	hydrogen is available and it is needed, it is possible to reduce infrastructure costs and transportation expenses. A comprehensive cost analysis comparing this approach to traditional hydrogen transport methods will provide valuable insights into its advantages, potentially offering a more sustainable and cost-effective solution while making the most of existing infrastructure originally designed for fossil fuels.
B	**Conference Proceeding(s)**
3.	Angle of arrival antenna array design for BLE 5.1 direction finding **R Raina, S Kumar** - 2024 International Symposium on Antennas and Propagation (ISAP), 2025 **Abstract:** Indoor localization is the procedure of determining the precise position of an object or person within a confined space, such as building or room. Unlike outdoor global positioning systems (GPS) that rely on satellite signals, indoor localization faces extra challenges because of the absence of reliable GPS signals in indoor environments. Directional finding systems in Bluetooth Low Energy (BLE) frequently utilize antenna arrays based on the Angle of Arrival (AoA) method to determine the source of a BLE signal. This technology is widely utilized in situations like indoor positioning, asset tracking and location-based services. Thus, in this regard, 12patch antenna array is proposed in this paper for direction finding applications. A 12-patch antenna array is designed and fabricated using an FR4 substrate measuring 200 mm X 200 mm with 1.6 mm thickness. Additionally, simulation and design of the 12-patch AoA antenna array are conducted using Ansys Electronics Desktop 2021R1. The A3 patch antenna operates in 2.37-2.49 GHz frequency band with 2.40 GHz resonant frequency. Moreover, it has -20.30 dB return loss and 3.2 dBi gain. Also, the simulated results closely align with the measured findings.
4.	Black hole search in dynamic graphs **T Kaur, A Saxena**, PS Mandal, **K Mondal** - ICDCN '25: Proceedings of the 26th International Conference on Distributed Computing and Networking, 2025 **Abstract:** A black hole is considered to be a dangerous node present in a graph that disposes of any resources that enter that node. Therefore, it is essential to find such a node in the graph. Let a group of agents be present on a graph G. The Black Hole Search (BHS) problem aims for at least one agent to survive and terminate after finding the black hole. This problem is already studied for specific dynamic graph classes such as rings, cactuses, and tori where finding the black hole means at least one agent needs to survive and terminate after knowing at least one edge associated with the black hole. In this work, we investigate the problem of BHS for general graphs. In the dynamic graph, adversary may remove edges at each round keeping the graph connected. We consider two cases: (a) at any round at most one edge can be removed (b) at any round at most f edges can be removed. For both scenarios, we study the problem when the agents start from a rooted initial configuration. We consider each agent has O(log n) memory and each node has O(log δv) storage. For case (a), we present an algorithm with 9 agents that solves the problem of BHS in O(|E|2) time where |E| is the number of edges and δv is the degree of the node v in G. We show it is impossible to solve for 2δBH many agents starting from an arbitrary configuration where δBH is the degree of the black hole in G. For case (b), we provide an algorithm using 6f agents to solve the problem of BHS, albeit taking exponential time. We also provide an impossibility result for 2f + 1 agents starting from a rooted initial configuration. This result holds even if unlimited storage is available on each node and the agents have infinite memory.
5.	Digital entomology sensor for advanced biodiversity monitoring and precision agriculture **M Kaur, S Kumar** - International Conference on Agriculture-Centric Computation (ICA 2024), 2025 **Abstract:** Insects comprise the majority of species on earth, but their population is facing a rapid

	decline. Many studies have highlighted the impact of excessive use of fertilizers and the effect of continuous change in farm practices on pollinator's biodiversity. To preserve their biodiversity, 24×7 monitoring of flying insects on farmland is essential. Manual observation-based traditional monitoring techniques are ineffective, time-consuming and not applicable for real-time field monitoring. To overcome these limitations, an idea is to develop a network of digital sensors on farmland for effective monitoring of biodiversity. This paper proposes the development of a Digital Entomology (DE) sensor for biodiversity surveillance at a large scale. The sensor monitors the real-time movement of airborne insects along with environmental data and processes it on the cloud for subsequent analysis. The proposed DE sensor is a solar-powered and IoT-enabled processor device suitable for deployment at remote locations. The local management of the sensor is facilitated through the Device Manager Portal (DMP) for accessing device configurations and enabling data downloads via a local Wi-Fi hotspot. The inclusion of over-the-air updates (OTA) capability enables the management and updates of sensors from a location that can be far away from where it is deployed. The proposed DE precisely detects the pollinator's movement with a high accuracy during testing in farmlands which makes it superior to other existing systems available in the market.
6.	Dispersion on time varying graphs **A Saxena, T Kaur, K Mondal** - ICDCN '25: Proceedings of the 26th International Conference on Distributed Computing and Networking, 2025 **Abstract:** The dispersion problem involves the coordination of $k \leq n$ agents on a graph of size n to reach a configuration where at each node at most one agent can be present. It is a well-studied problem on static graphs. Also, this problem is studied on dynamic graphs with n nodes where at each discrete time step the graph is a connected sub-graph of the complete graph K_n. An optimal algorithm is provided assuming global communication and 1-hop visibility of the agents. How this problem pans out on Time-Varying Graphs (TVG) is kept as an open question in the literature. In this work we study this problem on TVG where at each discrete time step the graph is a connected sub-graph of an underlying graph G (known as a footprint) consisting of n nodes. We have the following results even if only at most one edge from G is missing in the connected sub-graph at any time step and all agents start from a rooted initial configuration. Even with unlimited memory at each agent and 1-hop visibility, it is impossible to solve dispersion on a TVG in the local communication model. Furthermore, even with unlimited memory at each agent but without 1-hop visibility, it is impossible to achieve dispersion in the global communication model. From the positive side, the existing algorithm for dispersion on dynamic graphs with the assumptions of global communication and 1-hop visibility works on TVGs as well. This fact and the impossibility results push us to come up with a modified definition of the dispersion problem on TVGs, namely the saturated dispersion problem, as one needs to start with more than n agents if the objective is to drop the strong assumptions of global communication and 1-hop visibility. Then we provide an algorithm to solve saturated dispersion on TVG starting with $n + 1$ agents with $O(\log n)$ memory per agent while dropping both the assumptions of global communication and 1-hop visibility. This algorithm is optimal with respect to memory per agent.
7.	KrishiAI: Architecture for harnessing capabilities of LLMs for delivery of accurate cultivation information to farmers **M Kumar**, S Wilson, **N Goel**, A Ginige - International Conference on Agriculture-Centric Computation (ICA 2024), 2025 **Abstract:** With the constantly evolving agricultural environment, farmers need timely information relevant to their context to make informed decisions. Although several digital solutions have been introduced to address this requirement, these disregard farmers' context in providing information, including information quality. To address this gap, we developed a chatbot in this study incorporating the latest advances in computing techniques. We created an architecture to harness current Large Language Model (LLM) capabilities, including knowledge

	modeling, to deliver context-specific information to users through questions and answers. The context was established from previous interactions in the form of a dialogue. Neo4J graph database was used to create the knowledge base, ensuring efficient storage and retrieval of contextual information. LLM was used to convert user queries into Cypher queries and to transform knowledge base responses into natural language. A sanitiser module was developed to verify the accuracy of the Cypher queries generated through LLM, significantly enhancing the system's overall reliability. The primary evaluation proved that transitioning from a traditional document-based format to a question-and-answering format and then to a dialogue-based format significantly enhances farmers' ability to access the desired information effectively and promptly.
8.	Luminate: Linguistic understanding and multi-granularity interaction for video object segmentation **R Tekchandani, R Maheshwari, P Hambarde**, SN Tazi, **SK Vipparthi**, S Murala - 2024 IEEE International Conference on Image Processing (ICIP), 2024 **Abstract:** Referring Video Object Segmentation (R-VOS) is a challenging task that involves segmenting objects in a video based on linguistic descriptions. In this paper, we introduce a novel multi-granularity referring video Object segmentation framework, termed as LUMINATE. The LUMINATE framework introduces a streamlined approach to cross-modal fusion. The proposed LUMINATE enhanced interaction between visual and textual modalities begins with cross-attention between the vision encoder's query and the text encoder's key-value pairs, and vice versa. The results are then concatenated with the respective queries of the vision and text encoders, fostering a comprehensive understanding of semantic relationships. The combined features are fed into the Transformer Encoder for further refinement and integration into the segmentation pipeline. Extensive experiments on benchmark datasets, including Ref-DAVIS, demonstrate that our proposed LUMINATE approach achieves better results than state-of-the-art methods in terms of Jaccard and F-measure evaluation metrics. Furthermore, the efficiency of our multi-object R-VOS variant is highlighted, achieving a threefold speed improvement while maintaining satisfactory segmentation performance. The proposed approach contributes to advancing the capabilities of R-VOS models, paving the way for improved multimodal reasoning and real-world applications.
9.	Numerical simulation and flow modeling of viscoelastic fluid for heat transfer enhancement applications C Mathur, **C Sasmal**, P Kodgire - Computational Modeling and Sustainable Energy (ICCMSE 2023), 2025 **Abstract:** The current study demonstrates a detailed analysis of heat transfer enhancement characteristics of a viscoelastic fluid using the finite volume method (FVM) based Open-source computational fluid dynamics (CFD) code OpenFOAM, from a heated circular cylinder immersed in it. The Oldroyd-B viscoelastic consecutive equation models the fluid to study the constant-shear viscosity effect of viscoelastic fluid on flow dynamics. The numerical simulations were carried out over a range of dimensionless numbers, Weissenberg number ($0 \leq Wi \leq 100$), while maintaining fixed values for Reynolds ($Re = 5$ and 100), Prandtl numbers ($Pr = 0.7$), and polymer viscosity ratio ($ß = 0.5$). The results illustrate that at a high Weissenberg number, elastic turbulence arises in the systems, significantly altering the flow behavior and, thus, the heat transfer characteristics of the system. While the current study focuses on a simplified system, its findings can prove valuable in designing process equipment to enhance the heat transfer rate.
10.	RISC-V based secure processor architecture for return address protection **L Sharma, N Goel** - 2025 38th International Conference on VLSI Design and 2024 23rd International Conference on Embedded Systems (VLSID), 2025 **Abstract:** RISC-V-based cores are increasingly becoming pop-ular in embedded system

	applications because of their open-source architecture. Protecting such systems against memory-based attacks is one of the most difficult challenge. Buffer over-flow (BFO) attacks, specifically on Stack, can alter the program execution flow and are extensively employed by attackers. RISC-V foundation is working on specifications that will be used to maintain the control flow integrity (CFI) of the overall system. It will add 'zicfiss' and 'zicfiip' extensions for both backward edge and forwarded edge CFI, respectively. We propose a hardware-based approach that uses existing Return Address Stack (RAS) and requires low overhead, minimal microarchitecture changes, and limited software overhead to protect against such attacks. We assessed the performance of our design using buffer-intensive benchmarks. We verified its security by subjecting it to evaluation with the RIPE benchmark and our in-house test cases for BFO check. This approach safeguards the system from BFO attacks and could also enhance its security against Spectre attacks that exploit RAS vulnerabilities. We validated our design with Rocket-Core-based SoC and found less than 0.1% memory overhead and 2% timing overhead from the best case.
11.	Security analysis and implementation strategy for (E-Rupi) digital mobile wallet development **S Apraj**, V Rohokale, R Prasad - 2024 27th International Symposium on Wireless Personal Multimedia Communications (WPMC), 2025 **Abstract:** This paper discusses security analysis and implementation strategy for the E-Rupi Digital Wallet application. The platform DigiRupi requires to be easy, safe & secure as it keeps the details of the beneficiaries completely confidential. This seamless one-time payment mechanism enables users to redeem the voucher without a card, by means of a digital payments app. It needs to be secured from all aspects of Security threats like Access Control, Confidentiality, Authentication, Reputation, Integrity, Accuracy and Availability. We looked at regulatory compliances, trends.
12.	Semi-automated ground truth generation system for bangla offline handwritten text documents **R Chakraborty**, P Rakshit, C Halder, K Roy - Applied Computing for Software and Smart Systems: Proceedings of ACSS 2024, 2025 **Abstract:** In the field of image processing, document-level image processing is one of the trending topics. Various researchers have proposed works on Bangla handwritten documents, and one of them is segmentation and ground truth generation. Segmentation schemes for lines, words, and characters are a crucial preprocessing task in many applications. Segmentation algorithms for Bangla handwritten offline documents that have been proposed so far were unable to achieve significantly high accuracy due to various problems like overlapping of components, cut-through, etc. Fully manual segmentation can produce highly accurate results but it is not feasible for any user. In this paper, a semi-automated system has been proposed for Bangla handwritten documents which can potentially produce fully accurate segmentation results. Furthermore, ground truth generation for words has also been added to the system using the isolated character recognition CNN model.
C	**Journal Article(s)**
13.	A compact planar multisector rectenna array with full-wave rectification for 3D uniform wireless powering of IoT nodes **M Kumar, A Sharma** - IEEE Transactions on Antennas and Propagation, 2025 **Abstract:** Microwave power transfer offers a promising solution for wirelessly charging sensor nodes in Internet-of-Things (IoT) applications. However, conventional rectennas suffer from limited power harvesting area and significant dependence on sensor node orientation and location relative to the transmitter. This paper presents a novel planar multisector mirror rectenna array designed for efficient and uniform microwave power transfer to wirelessly charge IoT sensor nodes. The proposed system addresses limited power harvesting challenges by integrating four radially arranged end-fire (EFRA) elements surrounding a centrally located bore-sight (BSRA)

	element on both sides of the array like a mirror, ensuring orientation-insensitive coverage in both azimuth and elevation planes. The design facilitates direct conjugate matching of the antenna and rectifier circuit, minimizing insertion losses and enabling a compact, fully integrated form factor. This configuration provides isotropic coverage, making it ideal for RF wave-constrained IoT environments. Simulation results indicate that the system achieves a notable RF-DC conversion efficiency, with the maximum efficiency for the two-series combined EFRA elements observed at 64% (measured 60.5%) and a complete system efficiency of 55% at 2240 Ω and 44.76% at 2482 Ω for $\theta = 90^\circ$ and $\phi = 0^\circ$ planes, respectively. The SDRS system can harvest approximately 1600 mV of open DC voltage, sufficient to recharge and operate low-power IoT sensor nodes. The experimental setup validated these results, demonstrating the system's potential as a robust solution for wireless power transfer in smart environments.
14.	A novel power theft and data breach detection technique for low-voltage distribution networks **S Agarwal, R Sodhi** - Electric Power Systems Research, 2025 **Abstract:** Monitoring the security and integrity of smart meters is essential to combat power theft issues. To this end, this paper proposes a novel Dynamic Power Theft and Data Breach Detection technique for low-voltage distribution networks. The Dynamic Power Theft and Data Breach Detection technique consists of two stages wherein Stage-1 evaluates feature combinations, and Stage-2 involves dynamic clustering of feature combinations. An advanced clustering algorithm called Dirichlet Process Mixture Modelling, based on a non-parametric hierarchical Bayesian model, is employed to distinguish tampered meters. The methodology developed is tested on real-life datasets, including Pecan Street's New York dataset and the UK power network's London dataset. The efficacy of the proposed technique is verified by comparing its performance after incorporating popular exploratory data analysis techniques such as Pearson Correlation Coefficient, Fuzzy C-Means, and Density-Based Spatial Clustering of Applications with Noise. The comparative evaluation focuses on calculating metrics such as Accuracy, Geometric Truth Rate, Youden's Index and Area under Receiver Operating Characteristics curve for each of these methods, alongside the proposed methodology. A rigorous analysis based on multiple trials conducted for each theft scenario reveals that the proposal achieves an overall Accuracy, Geometric truth rate, Youden's index of 91.72%, 91.67% and 83.34% on the Pecan data streets and 96.73%, 96.83% and 93.67% on the UK power networks, respectively. The results verify the effectiveness of the proposed technique in distinguishing tampered and non-tampered low-voltage distribution network consumers.
15.	Additive manufacturing of styrene-isoprene-styrene block copolymer based soft thermoplastic elastomeric nanocomposites: Influence of reduced graphene oxide on microstructural, mechanical and functional properties A Kumar… PM Pandey, **C Sasmal**, SS Banerjee - Macromolecular Chemistry and Physics, 2025 **Abstract:** Additive manufacturing enables the customization of parts according to user requirements. However, additive manufacturing of soft polymeric materials using melt-based fused deposition modeling is challenging due to issues such as low column strength, high melt viscosity, poor adhesion with the print bed, and weak layer-to-layer adhesion. This work focused on the development of soft thermoplastic elastomeric nanocomposite materials based on reduced graphene oxide (rGO) and styrene-isoprene-styrene (SIS) triblock copolymer by direct ink writing (DIW) based additive manufacturing technique. The extrudability and printability of the developed SIS-rGO inks with varying rGO loading are investigated from shear viscosity and pressure drop analysis across different zones of the nozzle. Developed 3D printed nanocomposites showed good mechanical properties such as high elongation at break (≥ 2000%) and high tensile strength (5–11 MPa). Microstructures of 3D printed samples and the distribution of rGO nanosheets in the SIS matrix are analyzed from XRD and TEM. Dielectric constant of 3D printed nanocomposites increased ≈6 times for the 7 wt.% loaded rGO nanocomposite compared to the pristine SIS. Additionally, the electromagnetic interference shielding effectiveness (EMI

	SE) by absorption is also found to increase with rGO loading in the 3D-printed samples.
16.	Advancements in cache management: A review of machine learning innovations for enhanced performance and security **K Krishna** - Frontiers in Artificial Intelligence **Abstract:** Machine learning techniques have emerged as a promising tool for efficient cache management, helping optimize cache performance and fortify against security threats. The range of machine learning is vast, from reinforcement learning-based cache replacement policies to Long Short-Term Memory (LSTM) models predicting content characteristics for caching decisions. Diverse techniques such as imitation learning, reinforcement learning, and neural networks are extensively useful in cache-based attack detection, dynamic cache management, and content caching in edge networks. The versatility of machine learning techniques enables them to tackle various cache management challenges, from adapting to workload characteristics to improving cache hit rates in content delivery networks. A comprehensive review of various machine learning approaches for cache management is presented, which helps the community learn how machine learning is used to solve practical challenges in cache management. It includes reinforcement learning, deep learning, and imitation learning-driven cache replacement in hardware caches. Information on content caching strategies and dynamic cache management using various machine learning techniques in cloud and edge computing environments is also presented. Machine learning-driven methods to mitigate security threats in cache management have also been discussed.
17.	ALP-mimetic cyclic peptide nanotubes: A multifunctional strategy for osteogenesis and bone regeneration **V Chawla, P Bundel, Y Singh** - Biomacromolecules, 2025 **Abstract:** Alkaline phosphatase (ALP) plays a crucial role in bone mineralization by hydrolyzing organophosphates and releasing inorganic phosphate ions, facilitating hydroxyapatite formation. The imidazole ring in the functional domain of ALP is critical for its catalytic activity and bone mineralization. However, the therapeutic application of native ALP is hindered by instability, short half-life, immunogenicity, and variable efficacy. This work presents the development of ALP-mimetic cyclic-octapeptide (ALAKHKHP) nanotubes to promote osteogenic differentiation and bone mineralization. The incorporation of imidazole-rich histidine residues in close proximity gives enzyme-mimetic characteristics. The nanotubes effectively catalyzed *para*-nitrophenyl phosphate (*p*NPP) hydrolysis, promoting *in vitro* calcium deposition and ALP activity, which stimulated osteogenic differentiation of MC3T3-E1 preosteoblasts, as evidenced by the upregulation of osteogenic marker genes. The nanotubes demonstrated excellent cell migration, reactive oxygen species (ROS) scavenging, and anti-inflammatory properties. This biomimetic nanoscaffold provides a promising alternative for bone regeneration, without relying on native enzymes, growth factors, or drugs. 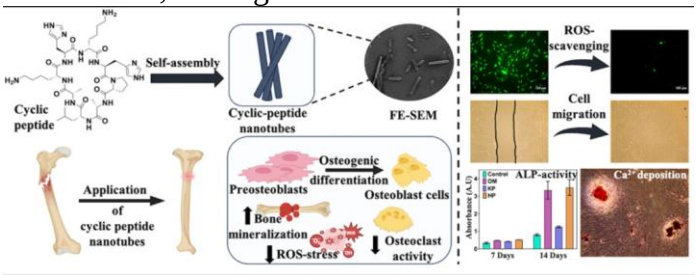
18.	An adaptive fractional voltage MPPT with the exponential sliding AC voltage and current controllers for enhanced power processing integrity **A Kumar, BK Gupta, AS Kiran, KR Sekhar** - IEEE Transactions on Industry Applications, 2025

	Abstract: In this work, a novel adaptive fractional open circuit voltage (AFOCV) MPPT algorithm is devised for a grid-connected inverter, aiming to optimize power processing integrity and enhance energy yield amid fluctuating irradiance and temperature. The proposed algorithm incorporates adaptive solar constant updates to accommodate environmental uncertainty. Additionally, a novel control mechanism is introduced for voltage and current controllers to improve grid-injected current quality while minimizing voltage deviations on the DC side. This mechanism employs a modified exponential reaching law to approach the proposed sliding surface. The modified control tracks the voltage and current error based on the designed sliding surface to achieve the steady-state voltage and current reference. The proposed sliding surface additionally enhances coordination between inner and outer loops, ensuring smoother operation. It also improves dynamic response when tracking voltage and current references. Further, the effectiveness of the proposed algorithm, coupled with the novel controller, is compared with conventional methods, showcasing its superior performance under diverse environmental conditions. Moreover, the effectiveness of the AFOCV algorithm, coupled with the proposed controller for the solar grid-connected inverter, is experimentally validated on the developed prototype in the laboratory. This validation involves replicating various environmental conditions using a solar emulator.
19.	Analytical model for transient space charge in low density polyethylene **P Muppala, CC Reddy** - IEEE Transactions on Dielectrics and Electrical Insulation, 2025 **Abstract:** Despite being an experimentally well-studied phenomena, a consistent lacuna has always persisted in the theoretical and mathematical understanding of space charge dynamics in LDPE. The macroscopic models reported so far in the literature seem to be insufficient and fail to predict the formation of homo and hetero charges near the electrodes and transport of charge packets. On the other hand, while microscopic models such as bipolar charge transport model were able to explain homo charge accumulation and movement of charge packets to a limited success, they are often fraught with assumptions such as neglection of diffusion phenomena and are structurally complicated when compared to macroscopic models. In this work, the authors have derived analytical solutions for space charge dynamics based on Maxwell's equations and Transient Space Charge Limited Current (TSLC) based volumetric current models, which takes into consideration the measured absorption (slow polarization) and steady state volumetric currents. The proposed analytical (macroscopic) model can thus predict the homo and hetero charge accumulation in LDPE, which is validated through comparisons with the experimentally measured space charge, wherein a remarkable agreement was observed. Furthermore, the relation between the transient volumetric current and space charge dynamics is reaffirmed.
20.	Aqueous Zn-ORR/CER battery in tandem electrolyte utilizing dual-function Ag catalyst **S Kaur, K Garg, TC Nagaiah** - ACS Energy Letters, 2025 **Abstract:** Amidst ever-growing energy demands, the development of efficient energy storage devices for carrying out a sustainable electrocatalytic reaction along with energy storage has proven to be viable. In this work, we report a Zn-ORR/CER battery in a tandem electrolyte for the first time, wherein a cost-effective silver (Ag) catalyst was used as a bifunctional electrocatalyst. It exhibits exceptional stability performance in mimicked industrial conditions, even under multiple shutdowns in chlorine-rich electrolytes. Moreover, the local electrocatalytic activity for ORR and the stability of the catalyst in a chlorine-rich electrolyte were probed through scanning electrochemical microscopy (SECM). Interestingly, when employed as a cathode for the Zn-ORR/CER battery (which runs on the electrocatalytic ORR and CER), it displays an open circuit voltage of 1.6 V with outstanding long-term stability for 380 cycles @ 10 mA cm^{-2}. The proposed Zn-ORR/CER battery exhibits a power density of 4.84 mW cm^{-2} with efficient chlorine production (75%) during charging.

	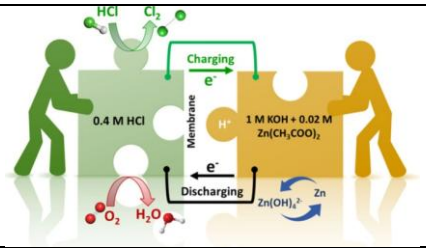
21.	Boundary carrollian conformal field theories and open null strings A Bagchi, **P Chakraborty, S Chakrabortty**, S Fredenhagen, D Grumiller, P Pandit - Physical Review Letters, 2025 **Abstract:** We consider Carrollian conformal field theories in two dimensions and construct the boundary Carrollian conformal algebra (BCCA), opening up innumerable possibilities for further studies, given the growing relevance of Carrollian symmetries. We prove that the BCCA emerges by contracting a single copy of the Virasoro algebra. As an application, we construct, for the first time, open null strings and show that, for Dirichlet boundary conditions, we recover the BCCA as the algebra of constraints. We finally reconstruct our string results by taking the null limit of tensile open strings.
22.	BPS2025 - Impact of differential stapling on peptide recognition and dynamics S Tolani, **NM Tripathi**, D Mitra, **A Bandyopadhyay**, A Kumar - Biophysical Journal, 2025 **Abstract:** Peptides have emerged as ambitious agents to target challenging protein-protein interaction (PPI) Interface. Modifications in peptide sequence and structure are routinely employed to make them amenable to the desired target. In our efforts to target the interface between Skp1-Skp2, a crucial PPI in cancer progression, we rationally designed a few peptides. Additionally, two exclusive stapling strategies were employed to improve the stability and potency of the peptides towards the interface. The effective changes in peptide dynamics caused by the stapling and its association with affinity against the target were highlighted through the concurrent use of surface plasmon resonance (SPR) and nuclear magnetic resonance (NMR) spectroscopy. Correlated associations of NMR relaxation parameters and chemical shift perturbations with affinity against the target highlight our efforts at decoupling enthalpic and entropic contributions through association and stapling. We aim to exploit our current understanding of the changing dynamics and its subsequent effect on peptide activity to develop an effective peptide inhibitor against our target of interest and extend our approach to equally challenging interfaces.
23.	Buckling instability mediated wetting behavior of low-energy ion irradiated polydimethylsiloxane (PDMS) films **P Kumar, D Rani**, S Bera, **M Sabapathy, S Sarkar** - Applied Surface Science, 2025 **Abstract:** Patterned polymeric surfaces play a crucial role in advanced application areas of biomedical engineering, flexible devices, and tunable optics. In this study, we explore the evolving surface pattern, in particular the wrinkle morphology, and the associated wetting properties of polydimethylsiloxane (PDMS) surfaces under low-energy Ar+ ion beam irradiation. Our results have been explained in the light of an apropos localized deformation theory in contrast to the linear collision cascade model usually employed for ion sputtered surfaces. We show that the wavelength and amplitude of the wrinkle patterns can be efficiently tuned by changing the ion incidence angle. X-ray photoelectron spectroscopy (XPS) studies further confirm the formation of a stiff silica-like top layer across the penetration depth of the impinging Ar+ ions. The localized deformation theory is valid below a critical thickness of this layer while structuring through the cascade model is applicable above it. Structural investigations further suggested an alteration of crystallinity and polymer chain alignment with ion irradiation. Water contact angle measurements performed on the compressive-strain induced buckled surfaces

	demonstrated systemic variations in surface wettability as a function of the incidence angle. Our investigations establish a method for patterning polymer surfaces with controlled periodicity and surface wettability with potential applications in various fields.
24.	Combined effects of fluid elasticity and plasticity on flow past a rotating circular cylinder **S Raffi, A Chauhan, C Sasmal** - Physics of Fluids, 2025 **Abstract:** The flow past a rotating cylinder is a classic benchmark problem in the domain of fluid dynamics, extensively studied in the past through experiments and numerical simulations. However, most prior research has focused on simple Newtonian fluids. In contrast, many fluids encountered in practical applications display complex non-Newtonian characteristics, such as elasticity and plasticity. This study presents a numerical investigation into the influence of these non-Newtonian properties on the flow dynamics around a rotating circular cylinder within the laminar vortex-shedding regime. Simulations are performed at a fixed Reynolds number (Re=100), exploring a wide range of Weissenberg numbers ($0 \leq Wi \leq 5$), Bingham numbers ($0 \leq Bn \leq 1$), and cylinder rotational speeds ($0 \leq \Omega \leq 1$). The Saramito constitutive model is employed in this study to capture the combined effects of fluid elasticity and plasticity. Results indicate that both the fluid's non-Newtonian behavior and cylinder rotation significantly alter the flow characteristics. For instance, the vortex-shedding frequency downstream of the cylinder decreases with increasing Wi and Bn, showing minimal change beyond critical values in the case of a rotating cylinder. In contrast, for a fixed cylinder, the vortex-shedding frequency initially decreases and subsequently increases at higher Wi. Additionally, the time-averaged drag coefficient increases with both Wi and Bn, while the root mean square lift coefficient decreases both for fixed and rotating cylinders. However, the variation in lift coefficient with Bn is minimal for the rotating cylinder. The flow structures downstream of the cylinder also exhibit distinct patterns. For instance, at high Wi, the streamlines become highly distorted and broken for a fixed cylinder but remain more ordered for a rotating cylinder. Most importantly, the present study finds a transition of the flow field from regular periodic behavior to irregular aperiodic one at higher Wi, observed for both fixed and rotating cylinders in elastoviscoplastic (EVP) fluids. This transition highlights the increased complexity of flow dynamics in EVP fluids compared to Newtonian fluids under identical flow conditions. This needs to be understood thoroughly, particularly in applications involving non-Newtonian fluids, where accurate predictions of flow behavior are essential.
25.	Condensate droplet roaming on nanostructured superhydrophobic surfaces CWE Lam, K Regulagadda, M Donati, A Tripathy, **GC Pal, CS Sharma**, A Milionis, D Poulikakos - Nature Communications, 2025 **Abstract:** Jumping of coalescing condensate droplets from superhydrophobic surfaces is an interesting phenomenon which yields marked heat transfer enhancement over the more explored gravity-driven droplet removal mode in surface condensation, a phase change process of central interest to applications ranging from energy to water harvesting. However, when condensate microdroplets coalesce, they can also spontaneously propel themselves omnidirectionally on the surface independent of gravity and grow by feeding from droplets they sweep along the way. Here we observe and explain the physics behind this phenomenon of roaming of coalescing condensate microdroplets on solely nanostructured superhydrophobic surfaces, where the microdroplets are orders of magnitude larger than the underlaying surface nanotexture. We quantify and show that it is the inherent asymmetries in droplet adhesion during condensation, arising from the stochastic nature of nucleation within the nanostructures, that generates the tangential momentum driving the roaming motion. Subsequent dewetting during this conversion initiates a vivid roaming and successive coalescence process, preventing condensate flooding of the surface, and enhancing surface renewal. Finally, we show that the more efficient conversion process of roaming from excess surface energy to kinetic energy results in significantly improved heat transfer efficiency over condensate droplet jumping, the mechanism currently understood as

	maximum.
26.	Contactless breathing monitoring at home and in the hospital: Protocol for a low-cost frequency-modulated continuous-wave radar-based device **A Hari, R Kumar, B Kumbhani, S Darshi, S Agarwal, JS Sahambi**… - JMIR Research Protocols, 2025 **Abstract:** Background: Contactless monitoring of vital signs, especially the breathing of children, in the hospital is performed on a priority basis because their organs and immune system are immature. Therefore, continuous monitoring of their vital signs with a sensor that is directly attached to their body is not possible, as it irritates the sensitive newborn skin and causes discomfort. A contactless frequency-modulated continuous-wave (FMCW) radar-based device can wirelessly monitor the breathing rate and pattern of a child in the hospital or at home. Signal-processing capability can be added to this device to process breathing data and analyze the apnea condition arising due to irregular breathing patterns. Objective: This study will develop a contactless FMCW radar-based system to accurately monitor the breathing rate and pattern of neonates and infants in hospitals and at home in order to provide a noninvasive, nonintrusive and contactless alternative to conventional sensor-based methods and address a critical need in neonatal care, potentially improving health outcomes for vulnerable infants. Methods: The radar transmits a signal toward the body, and the time taken by the signal received to travel from the body to the receiving antenna is analyzed. This time is proportional to the distance between the radar and the body, and the breathing pattern is recognized as a slight, periodic variation in this distance. We will use this concept with multiple antenna systems to monitor the breathing of neonates with improved sensitivity. The radar-based device will be installed, in addition to conventional breathing monitors, in the neonatal intensive care unit. The signals received at the radar and the respiration signals from conventional monitors will be recorded in a database. Signal-processing techniques will be applied to extract breathing signals from the signals received at the radar. Results: This study was funded in January 2023 by the Science and Engineering Research Board (SERB) of India. The device was designed by May 2024, and a working proof-of concept was verified in the Indian Institute of Technology (IIT) Ropar laboratory. Implementation of the proposed method for initial study began in December 2024. Results are expected to be published in the first quarter of 2025. Conclusions: The contactless FMCW radar-based system will provide reliable estimation of the breathing rate and pattern, which is close to the conventional reference device values most of the time. Our device will also provide a seamless breathing-monitoring system to be used both in hospitals and at home for newborns and premature babies until they are fully healthy and fit.
27.	Crack control in dried ferro-colloidal droplets: Effect of particle aspect-ratio and magnetic field orientations **D Rani, S Sarkar** - Physical Chemistry Chemical Physics, 2025 **Abstract:** Crack formation in dried colloidal films is a common phenomenon encountered in diverse fields, from coatings and materials science to biological and environmental applications. Understanding the mechanisms behind crack patterns and their dependency on external factors is crucial for tailoring deposit structures. In this study, we investigate the impact of an externally directed magnetic field on the crack morphology and self-assembly in dried deposits composed of anisotropically shaped ferro-colloidal particles of varying sizes. Employing a sessile drop configuration, distinct crack patterns are observed in ring-like deposits as the magnetic field is applied in parallel, perpendicular, and oblique orientations. Notably, crack propagation in the oblique field direction transitions from wavy to helical-shaped patterns depending on the size of the nanoparticles, in contrast to the patterns seen in parallel and perpendicular fields. Our findings demonstrate that ferro-colloids align with the magnetic moment along the tensile stress direction, particularly at the edges of the deposits where cracks propagate. The particle orientation and self-assembly in the deposits were controlled by the interaction of hydrodynamic

	and magnetic forces, with force calculations revealing that this interaction strongly depends on particle size and field angle. This interaction leads to crack alignment along the particle's long axes, emphasizing the influence of the magnetic field on the deposit's structural integrity. Additionally, ferro-colloid concentration significantly impacts crack density, with higher concentrations promoting the development of prominent cracks at the rim edges of the deposits. By leveraging the interplay between magnetic interactions and evaporation dynamics, we can develop novel strategies for manipulating nanoscale structures for advanced technology. 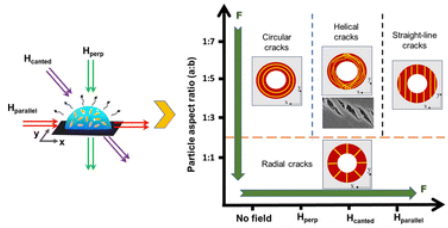
28.	Dynamics of shear instability in A+B→C reactive flow yielding high-viscosity products **SN Maharana, M Mishra** - International Journal of Multiphase Flow, 2025 **Abstract:** This numerical study investigates shear instabilities in a two-layered reactive system within a 2D channel, governed by the Navier–Stokes equations. Examining laminar Poiseuille flow, we explore the shearing of reactant fluids A and B, undergoing the A+B→C reaction. The favorable shear due to increased viscosity of the product fluid C amplifies periodic perturbations, forming roll-ups resembling interfacial waves. Increased Reynolds number leads to ligament formation. Vorticity field strength correlates with product fluid viscosity, enhancing instability growth. In the stable flow regime, the streamlines initially remain horizontally straight, but they start oscillating synchronously for a favorable viscosity ratio, which amplifies the growth of roll-ups in the unstable regime. A nonlinear energy budget analysis reveals that the growth of the shear instability primarily arises from the energy contributions of axial and vertical convection, rather than from the reaction source or diffusion terms. Shear instability induces opposite transverse motion of the reaction rate and product center of mass. Measurement of transverse spreading reveals an intermediate convection-dominated time regime in unstable flow, interspersed with diffusion-dominated early and later regimes. Proximity of the reactive zone to the bottom wall induces streamlines to shift out of phase, forming humps, and changing the wavelength of perturbations with a delayed intermediate convection-dominated regime. 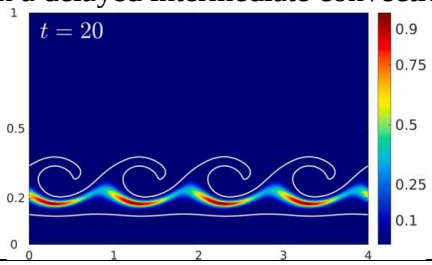
29.	Economical 550 V energy harvesting from plastic and electronic waste using human motions **M Singh, S Kumar, A Kafle, K Garg, P Sharma, CC Reddy, TC Nagaiah** - Journal of Materials Chemistry A, 2025 **Abstract:** Waste management of plastic and electronic artefacts is a very tedious task and requires a great deal of expense. The pressing threat to the environment due to excessive plastic use and uncategorized electronic waste management demands versatile strategies to mitigate the mentioned issues. Herein, we have showcased a very economical and straightforward approach to utilize plastic and electronic waste for designing a triboelectric nanogenerator (TENG). Polyethylene terephthalate (PET) recovered from used Kapton tape and, printing paper were utilized as triboelectric layers. More importantly, for the fabrication of the electrode layers,

	sophisticated and expansive techniques were replaced by a simple sacrificial electrodeposition of copper. Discarded electric wires from damaged UPS batteries were used as the source of copper. The fabricated TENG delivered excellent electric output with a maximum open circuit voltage of ~552 V, a short circuit current of 18.8 μA and a high-power density of 7.68 W m^{-2} under contact-separation triggered by human hand tapping. Additionally, the device exhibited a high open-circuit voltage of 615 V under vertical contact-separation driven by a custom-built linear motor, which is approximately 2 and 4 times greater than that of the TENG devices fabricated with Cu-tape and carbon electrodes, respectively. A vast number of practical demonstrations include the successful lighting of 472 LEDs connected in series, storing the charges in commercial capacitors, and powering a digital calculator. Furthermore, we demonstrated the potential application of e-Cu@WPP-TENG to power LED panels for advertisement boards, logos, nameplates, and similar displays in hotels, restaurants, buildings, laboratories, and homes. We believe that this work stresses the importance of implementing economically viable strategies for utilizing plastic and electronic waste to harvest valuable energy.
30.	Effect of electrolytes on electrical charge storage performance in a compost-based symmetric device Poonam, V Kumar, S Yadav, Chetan, Gauri, S Gupta, RK Choubey, S Gaurav, TK Gupta, **R Ahuja**, S Kumar - Applied Physics A, 2025 **Abstract:** The prevalence of compost and its integration within the bio-circular economy, facilitating the seamless conversion of bio-waste into compost, present an auspicious avenue for the exploration of renewable energy storage solutions. Thus, the current study investigates the effect of electrolytes on faradic and non-faradic processes of charge storage in a symmetrical device design based on compost. The inquiry examines the composts as an electrode material and the influence of various current collectors (G–G, Cu–Cu and IN–IN) across distinct aqueous electrolyte environments (1 M KNO_3, 1 M KCl and 1 M KOH). The findings reveal the composts' capacity to accommodate both capacitive and non-capacitive charge storage processes within a symmetric dual-current collector apparatus, showcasing the multifaceted charge storage modalities akin to those observed in capacitors and batteries. The electrochemical assessments, conducted through cyclic voltammetry (CV), galvanostatic charge–discharge (GCD) profiling, and electrochemical impedance spectroscopy (EIS), elucidate the non-faradaic and faradaic charge storage mechanisms in terms of the charge storage efficiency, temporal characteristics of the charge and discharge cycle, specific capacitance, and specific capacity. The results obtained evince the superior charge storage capabilities of the compost samples across various electrolyte solutions relative to the aqueous media. The compost specimen featuring a C:N ratio of 145.44 in a 1 M KCl solution assembled in a symmetric G–G current collectors device exhibited the optimal electrochemical performance. At a scan rate of 100 mV/s within a potential window of ± 4.5 V, the CV studies exhibited an area under the curve of 3.3142C, a specific capacitance of 18.4mF/g and a specific capacity of 82.8 mC/g, while the GCD studies were characterised by a charging time of 51 s, a discharging time of 47.2 s, a specific capacitance of 10.4 mF/g and a specific capacity of 94.4 mC/g at an applied current of 400 mA within a potential window of ± 4.5 V.
31.	Effect of reinforcement corrosion and axial load levels on seismic response of non-ductile reinforced concrete columns **SN Amini, AS Rajput** - Structural Concrete, 2025 **Abstract:** The present study investigated the seismic response of nonseismically designed reinforced concrete (NSRC) columns affected by varying degrees of reinforcement corrosion and subjected to different axial compression ratios (ACR). 3D numerical models representing corroded and noncorroded field-scale NSRC columns were developed and validated with experimental results. Subsequently, a parametric study was carried out to quantify the combined effect of different ACRs ($0.35P_0$, $0.5P_0$, $0.6P_0$, and $0.7P_0$) and corrosion degrees (0%, 15%, and

	30%) on the seismic response of NSRC columns. Critical parameters such as stiffness degradation, hysteresis backbones, ductility ratios, and energy dissipation were evaluated and compared for all the specimens. Results showed that the specimen corresponding to 15% corrosion and $0.7P_0$ ACR experienced a loss of flexural strength, ductility, and energy dissipation by alarming 55.2%, 60.6%, and 91.3%, respectively. The losses were even higher for specimens subjected to a 30% corrosion level. The quantification of catastrophic performance degradation in corrosion-affected NSRC columns provides crucial insights for designing effective retrofitting strategies to enhance their seismic resilience.
32.	Effect of sinusoidal injection velocity on miscible thermo-viscous fingering in a rectilinear Hele-Shaw cell S Zahid, SS Halkarni, P Das, TK Hota, **D Goyal** - Physics of Fluids, 2025 **Abstract:** This study examines the impact of sinusoidal time-dependent injection velocities on miscible thermo-viscous fingering instabilities observed in enhanced oil recovery. Linear stability analysis (LSA) and nonlinear simulations (NLS) are used to investigate fingering dynamics, considering parameters such as thermal mobility ratio ($R\theta$), solutal mobility ratio (Rc), Lewis number (Le), and thermal-lag coefficient (λ). The LSA employs a quasi-steady state approximation in a transformed self-similar coordinate system, while NLS uses a finite element solver. Two injection scenarios are explored: injection-extraction ($\Gamma=2$) and extraction-injection ($\Gamma=-2$), with fixed periodicity ($T=100$). Results show that for unstable solutal and thermal fronts ($Rc>0, R\theta>0$), increasing Le with fixed $\lambda \neq 1$ leads to more prominent mixing and interfacial length for $\Gamma=2$ compared to constant injection and $\Gamma=-2$. While for unstable solutal fronts ($Rc>0$) and stable thermal fronts ($R\theta<0$), increasing Le results in more prominent mixing and interfacial length for $\Gamma=-2$, except during early diffusion. Thus, when porous media are swept using cold fluid, increasing the Lewis number intensifies the level of flow instability for $\Gamma=-2$; whereas when hot fluid is used, the instability enhances for $\Gamma=2$. Furthermore, it is observed that the high thermal diffusion ($Le \gg 1$) and enhanced thermal redistribution between solid and fluid phases ($\lambda \ll 1$) effectively mitigate destabilizing effects associated with positive $R\theta$, reducing overall instability. Overall, in extraction-injection scenarios, the phenomenon of tip-splitting and coalescence is attenuated, and the channeling regime is observed.
33.	Efficient PMU data compression using enhanced graph filtering enabled principal component analysis **M Pandit, R Sodhi** - IEEE Transactions on Knowledge and Data Engineering, 2025 **Abstract:** Phasor Measurement Units (PMUs) are state-of-the-art measuring devices that capture high-resolution time-synchronized voltage and current phasor measurements in wide area monitoring systems (WAMS). Their usage for various real-time applications demands a huge amount of data collected from multiple PMUs to be transmitted from the local phasor data concentrator (PDC) to the control centre. To optimize the requirements of bandwidth to transmit the data as well as to store the data, an efficient synchrophasor data compression technique is desired. To this end, this paper presents a 3-stage data compression scheme in which Stage-1 performs the accumulation of the data matrix from the optimally placed PMUs in WAMS into the local PDC. The data is then passed through a novel Ramanujan's sum-based fault window detection algorithm to identify the fault within the PMU data matrix in Stage-2. Finally, Stage-3 proposes an enhanced graph filtering-enabled principal component analysis scheme which expands the notion of conventional PCA techniques into the graph domain to compress the data. The performance of the proposed scheme is verified on the IEEE 14-bus system and New England 39-bus system. Further, practical applicability of the proposed method is validated on field PMU data collected from EPFL campus in Switzerland.
34.	Enhancing battery thermal management: Magnetic nanofluid cooling with external magnetic field

	effects S Bhattacharyya, **A Aggarwal, A Aggarwal** - Journal of Thermal Analysis and Calorimetry, 2025 **Abstract:** The study aims to improve heat transfer in a heated mini-channel operating in the laminar regime by utilizing an external magnetic field together with a magnetic nanofluid containing CuO particles distributed in water to cool the batteries of electric vehicles (EV). The study was conducted for Reynold number ranging from 120 to 2000. In addition, the magnetic field intensity was adjusted to identify the optimal value that should be implemented. The magnetic field intensities were varied from 1000 to 2000 Gauss (G). Furthermore, the concentration of the CuO nanoparticles was also modified, ranging from 0 to 2% by volume fraction. The computational investigation, which involved varying parameters, revealed that the application of the magnetic field resulted in a maximum heat transfer enhancement of 127.96% when compared to that without the presence of a magnet for nanofluid as the working component. Moreover, the implementation of a magnetic field was observed to reduce pressure drop by 2–7%. However, a backflow was also observed in the channel flow following the application of the magnetic field. The formation of swirls in the flow, caused by the presence of magnets, contributed to the heat transfer augmentation. The thermal enhancement factor for all cases exceeded unity, providing evidence that the utilization of a magnetic field led to an improvement in heat transfer. The fundamental purpose of this study is to ensure that the EV batteries can operate at the utmost optimal temperature, thereby maximizing their overall performance of the system.
35.	Excitations of a supersolid annular stripe phase in a spin-orbital-angular-momentum-coupled spin-1 Bose-Einstein condensate **P Banger, Rajat, S Gautam** - Physical Review A, 2025 **Abstract:** We present a theoretical study of the collective excitations of the supersolid annular stripe phase of a spin-orbital-angular-momentum-coupled (SOAM-coupled) spin-1 Bose-Einstein condensate. The annular stripe phase simultaneously breaks two continuous symmetries, namely rotational and $U(1)$ gauge symmetry, and is more probable in the condensates with a larger orbital angular momentum transfer imparted by a pair of Laguerre-Gaussian beams than what has been considered in the recent experiments. Accordingly, we consider a SOAM-coupled spin-1 condensate with a $4\times\hbar$ orbital angular momentum transferred by the lasers. Depending on the values of the Raman coupling strength and quadratic Zeeman term, the condensate with realistic antiferromagnetic interactions supports three ground-state phases: the annular stripe, the vortex necklace, and the zero angular momentum phase. We numerically calculate the collective excitations of the condensate as a function of coupling and quadratic Zeeman field strengths for a fixed ratio of spin-dependent and spin-independent interaction strengths. At low Raman coupling strengths, we observe a direct transition from the zero angular momentum to the annular stripe phase, characterized by the softening of a double symmetric roton mode, which serves as a precursor to supersolidity.
36.	Exploring the potential of homologous epitopes from gut microbes for SARS-CoV-2 vaccine design, using molecular modelling to gain critical insights **S Prajapati, JA Malik, S Gupta, T Lamba, MA Zafar, MA Khan, S Nanda, Y Mehta, JN Agrewala** - Biologia, 2025 **Abstract:** This study addresses the role of gut microbiota in developing cross-reactive vaccines to protect against SARS-CoV-2. The gut microbiota positively influences lung diseases and is disrupted by respiratory infections. Exploring the interplay between gut microbes and SARS-CoV-2 is crucial. The gut is home to trillions of bacteria that release antigens that could cross-react with various pathogens. We aimed to identify T-cell and B-cell epitopes from gut microbiota and determine their potential cross-reactivity with SARS-CoV-2. We found that gut

	microbial species from Gamma proteobacteria and Bacillus classes show the highest similarity with SARS-CoV-2 proteins, suggesting these microbes are promising targets for epitope prediction and vaccine design. HLA-I and HLA-II epitopes demonstrated high promiscuity across multiple HLA alleles, enhancing their vaccine design potential. Immunogenicity assessments revealed that specific epitopes, like KITEHSWNA and QKALGGSVAIKITE, were highly immunogenic. The constructed vaccine exhibited stability, favorable physicochemical properties, and effective antigenicity. Structural validation, molecular docking, and molecular dynamics with TLR-4 confirmed the vaccine's potentials for immune activation. Immune simulations indicated robust immune responses, including significant IgM and IgG production and long-lasting memory B cells. This study highlights the potential of using cross-reactive epitopes from the gut microbiota to design effective vaccines, offering a promising strategy to enhance immune protection against SARS-CoV-2 and potentially other pathogens. © Plant Science and Biodiversity Centre, Slovak Academy of Sciences (SAS), Institute of Zoology, Slovak Academy of Sciences (SAS), Institute of Molecular Biology, Slovak Academy of Sciences (SAS) 2025.
37.	Functional Nanofibres of Tb(III)-Coupled Metal-Organic Gel: Detection To Decontamination of Thiabendazole In Environmental Samples **A Sharma**, N Kaur, **N Singh** - Chemistry–An Asian Journal, 2025 **Abstract:** Pollutant residues such as pharmaceuticals or pesticides in water bodies pose significant environmental and health risks, necessitating the development of advanced sensing and removal techniques to ensure safe and sustainable water resources. Tb-based luminescent sensors offer high sensitivity for pollutant residue analysis, but their application is often limited to detection. Developing Tb-derived metal-organic gel (ANS-4G-Tb) as soft supramolecular material is proposed to enhance trace contamination removal, integrating both sensing and sequestration capabilities. For the development of the self-assembled supramolecular material, ANS-4, a low molecular-mass organic gelator (LMOG) with a molecular weight of just about 215 g/mole, was selected, owing to its efficient single-step synthesis, and it was comprehensively characterized using single crystal XRD, and other routine spectroscopic techniques. Then, its nanosized ANS-4G-Tb metallogel was characterized using a comprehensive suite of analytical techniques to assess its structural, chemical, morphological, and optical characteristics. Upon interaction with parasiticide and fungicide thiabendazole (TBZ), a phase transformation from gel to sol is observed, enabling naked-eye detection and simultaneous turn-on photo-luminescence sensing ($^5D_4 \rightarrow {}^7F_5$ transition). Based on novel research, our study navigates through the photo-luminescence of lanthanide supramolecular complexes, transitioning from fundamental investigations to potential methodologies concerning analyte responsiveness and removal applications.
38.	Geometrically nonlinear analysis of composite plates through asymptotically accurate isoenergetic theory **AK Pathak, SJ Singh, SS Padhee** - Composites Part A: Applied Science and Manufacturing, 2025 **Abstract:** This study introduces a novel approach for analyzing composite plates. The methodology employs the Variational Asymptotic Method (VAM) in an innovative and mathematically rigorous manner to dimensionally reduce the plate using its three-dimensional (3D) model energy. The VAM decouples the 3D plate problem into a 1D through-the-thickness analysis and a 2D planar problem. The Through-the-thickness 1D analysis is done ensuring the continuity of displacements and transverse stresses. This elegantly reduces the dimension of the plate by expressing the 3D variables in terms of 2D variables. However, the obtained reduced-order model, while accurate, is not directly suitable for 2D extremization to solve for the remaining 2D variables. To address this challenge, Concept of isoenergetics is introduced, which eliminates higher-order derivatives, thereby facilitating efficient extremization and reducing

	computational complexities. The validity and versatility of our proposed methodology are demonstrated through comparisons with benchmark problems from the literature and 3D finite element analysis.
39.	Harnessing the efficiency of twin boron nitride and graphene monolayers for anticancer drug delivery: Insights from DFT B Roondhe, **R Ahuja**, W Luo - ACS Applied Bio Materials, 2025. **Abstract:** An extensive amount of research has been focused on the development of state-of-the-art methodologies for drug administration. In this study, we have utilized density functional theory (DFT) for assessing the ability of a Twin monolayer of boron nitride and graphene, i.e., Twin-BN and Twin-Gr monolayer, as a carrier for delivering four anticancer drugs (ACDs) 5-fluorouracil (5-FU), gemcitabine (GC), cyclophosphamide (CP), and mercaptopurine (6-MP). Also, the properties of all drug molecules along with the Twin-BN and Twin-Gr and the complex of the ACD-Twin-BN/Gr monolayer were investigated to explore the usefulness of the Twin-BN and Twin-Gr monolayer as ACD carrier. The interaction between the monolayers and ACDs confirmed that the adsorption is feasible as the adsorption energy ranged from −0.41 eV to −0.95 eV in the case of Twin-BN, while it ranged from −0.43 eV to −0.61 eV in the case of Twin-Gr. Additionally, the change in the band gap of the Twin-BN and Twin-Gr monolayers after the adsorption of ACDs was considerable. We can conclude that among both monolayers, Twin-BN can be utilized as a highly effective carrier for delivering ACDs. Our findings showed that the monolayer Twin-BN could be explored as a drug transporter for highly efficient carrying of the considered ACDs. 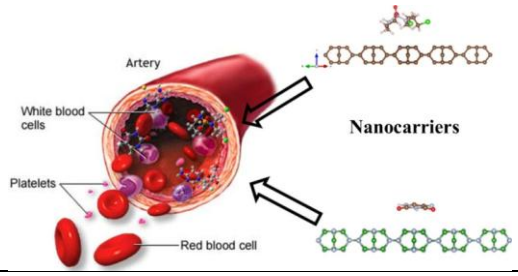
40.	High-performance VA-MoS_2/GO heterostructure-based sensor for in-situ soil moisture sensing **P Shukla, R Gond, B Rawat** - IEEE Sensors Letters, 2025 **Abstract:** This work presents a vertically aligned (VA)-MoS_2/graphene oxide (GO) heterostructure-based resistive sensor designed for high-performance soil moisture monitoring. The sensing film is fabricated using chemical vapor deposition (CVD) to grow VA-MoS_2 nanoflakes, followed by a spin coating of a colloidal GO solution. The sensor achieves a response of approximately 8.4% at 20% relative humidity (RH) and 41.18% at 80% RH, which demonstrates a broad detection range with high sensitivity. It also exhibits excellent stability, repeatability, and fast response and recovery times. In soil moisture measurement experiments, the sensor shows % responses of around 64.3, 139.8, and 160.67 for black soil with moisture contents of 5.9%, 16.2%, and 19.3%, respectively. With its wide sensing range, linear response, reliable performance, and cost-effective and scalable fabrication process, the VA-MoS_2/GO heterostructure holds great promise for next-generation soil moisture monitoring applications.
41.	Incorporation of phase change materials into building materials and envelopes for thermal comfort and energy optimization: A comprehensive review **PJ Abass, S Muthulingam** - Journal of Building Engineering, 2025 **Abstract:** Rising building energy use necessitates improved efficiency for sustainability and security. Phase Change Materials (PCMs) have emerged as a sustainable approach for passive building design. The review focuses on the growing need for sustainable buildings by exploring PCM integration techniques and their effects on thermal performance and energy savings. An

	extensive review was conducted on PCM classifications, incorporation methods, and their performance across various building envelopes and materials. Key findings show that PCM-enhanced building components help reduce indoor temperature fluctuations, cooling loads, and improve thermal comfort. Novel PCM encapsulation techniques, such as microencapsulation and composites, offer improved thermal stability and energy storage efficiency. The study emphasizes the importance of proper PCM placement and material selection to optimize performance. It provides insights into PCM integration challenges, future trends, and practical feasibility in real-world scenarios. This research offers a holistic analysis of PCM technologies, contributing to the development of energy-efficient and climate-resilient buildings, making it a valuable resource for researchers and practitioners in sustainable construction. 
42.	Instabilities in the blistering of two-dimensional materials **M Pandey**, G Wang, **G Singh, R Ahuja, R Kumar** - 2D Materials, 2025 **Abstract:** The blistering of two-dimensional (2D) materials is susceptible to elastic solid- or substrate-based mechanical instabilities. The phase transition of confined matter inside a circular blister or the interfacial slippage at the perimeter of the blister may give rise to wrinkling and tenting instabilities in 2D material blisters. Extensive research has focused on gaining adhesion mechanical insights of such instabilities in 2D material blisters over smooth, rigid substrates like silicon. These insights carry profound implications for quantum emission, magneto-straintronics, plasmonics, and piezotronics. In contrast, blistering a 2D material over a viscoelastic substrate has not received much attention. This gap has led to the underexploration of unconventional but fascinating phenomenon of viscous fingering in 2D materials, recently realized experimentally. Therefore, there is a significant demand for comprehending the formation and dynamics of instabilities in 2D material blisters, necessitating a critical review to advance this field. This understanding is key to either promoting or mitigating such instabilities, which has huge importance for both fundamental research and emerging quantum technologies.
43.	Investigation of gold-silicon eutectic bonding to realize the symmetric sensing element of MEMS piezoresistive accelerometer **S Singh**, V Kumar, SP Singh, **N Kumar** - IEEE Transactions on Components, Packaging and Manufacturing Technology, 2025 **Abstract:** In this paper, we investigate the intermixing of gold-silicon [Au-Si] across the Chromium [Cr] adhesion layer for Au-Si eutectic wafer bonding process development. In the first experiment, a stack of Cr and Au film was deposited on a silicon wafer, annealed in nitrogen gas ambient followed by the etching of unreacted Au, and investigated using optical microscopy, Scanning Electron Microscopy [SEM], and Energy-dispersive X-ray [EDX] analysis. The study confirms the intermixing and formation of Au-Si alloy. With that understanding, the Au-Si eutectic wafer bonding process was developed to realize a new symmetric sensing element for MEMS piezoresistive accelerometer. This structure is realized by bonding two silicon wafers containing complementary halves of the structure and Au-Au facing bond interface. Each half was formed by Deep Reactive Ion Etching [DRIE] in Silicon-On-Insulator [SOI] wafers. The DRIE-based method results in a smaller die size and eliminates the need for corner compensation, unlike KOH [Potassium hydroxide] or TMAH [Tetramethylammonium hydroxide] based wet etching of silicon, and it enables the fabrication of even a cylindrical seismic mass. Post bonding, the interface was investigated using SEM, high-resolution X-ray

	imaging and MIL-STD-883 based die shear test. The structure was successfully realized, achieving a 100% dicing yield of bonded wafers. For the 12 tested samples, the min, max, average, and standard deviation of die shear strength are 18.3, 40.1, 28.9, and 6.9 kgf, respectively. The average shear strength per unit of bond area is 27 MPa.
44.	Job insecurity and work engagement among teachers: Moderated-mediation involving affective well-being and emotion regulation difficulties **P Singh, S Kharwar, N Mishra** - Social Psychology of Education, 2025 **Abstract:** Enhancing teachers' work engagement requires systematic exploration of its contributors. Job insecurity has been considered a significant factor; however, other mediators and moderators may affect the relationship between job insecurity and work engagement. The present study tested a model of work engagement involving job insecurity as a predictor, affective well-being as a mediator, and emotion regulation difficulties as moderators of the mediational relationship. In this cross-sectional study, a total of 170 teachers (M_{age} = 32.22, SD_{age} = 7.83), selected using the purposive sampling technique, were assessed using standardized measures. The data were subjected to mediation and moderated mediation analysis. The analysis revealed that affective well-being mediates the relationship between job insecurity and work engagement, and emotion regulation difficulties moderate the effect of job insecurity on affective well-being. It implies that individuals with the same level of job insecurity but different levels of emotion regulation difficulties showed differences in their well-being and work engagement. Emotion regulation difficulties influence how job insecurity impacts work engagement. Job insecurity may not be a sufficient condition for reduced work engagement. It may be the difficulty in emotion regulation and consequent poor affective well-being due to heightened negative emotions that affect work-engagement. Helping teachers identify their emotion regulation difficulties and equipping them with functional and adaptive ER strategies may improve their work engagement.
45.	Li-doped 2D aza-fused covalent organic framework: A promising avenue for hydrogen storage **P Beniwal, TJ Dhilip Kumar** - Sustainable Energy & Fuels, 2025 **Abstract:** Designing an efficient high-capacity hydrogen storage material is a critical challenge for advancing clean energy storage. Through detailed density functional theory calculations and ab initio molecular dynamics simulations, we found that the recently synthesized two-dimensional (2D) aza-fused covalent organic framework (aza-COF) doped with Li exhibits considerable promise for hydrogen storage applications. Despite a H_2 storage capacity of 10.3 wt%, pristine aza-COF adsorbs H_2 molecules via weak van der Waals interactions, limiting its viability under ambient conditions. The strategy relies on increasing more active sites for H_2 adsorption, thereby improving the interactions between H_2 and positively charged Li atoms. Li-doped aza-COF adsorbs H_2 molecules with a combined effect of electrostatic and van der Waals interactions, resulting in enhanced H_2 adsorption energy, ranging from −0.22 to −0.33 eV. The H_2 storage capacity reaches 13.9 wt%, higher than that of the pristine aza-COF and the 5.5 wt% target of the U. S. Department of Energy. With appropriate structural stability, H_2 adsorption energy, desorption temperature, hydrogen occupation number and high H_2 storage ability, Li-doped 2D aza-COF exhibits great potential as a hydrogen storage material.
46.	Lyopreservation and nonionic decellularization of human amnion scaffolds for enhancing regeneration in chronic nonhealing ulcers **S Sarkar, JH Rajput, AA Poundarik** - ACS Applied Bio Materials, 2025 **Abstract:** Chronic nonhealing ulcers are responsible for considerable morbidity, given the increasing prevalence of type II diabetes and other comorbid conditions that further worsen healing. This study introduced shelf-stable decellularized and lyopreserved human amnion grafts for treating difficult-to-heal wounds. The processing approach (comprising a unique combination of nonionic surfactants and trehalose lyopreservation) applied to develop these bioscaffolds

	maximized the retention of sulfated glycosaminoglycans while enhancing both tensile property and hydrophilicity. Postprocessing, the tensile properties were found to be similar to human skin (5.33 ± 2.45 MPa). Additionally, the surface hydrophilicity of the lyopreserved grafts was increased. It also exhibited optimum moisture transmissibility (evaluated as per BS EN 13726–2 standards), similar to moist wound dressing (1625 ± 375 g/m^2/day). Biochemical attributes including total acid-soluble proteins (481.140 ± 14.95 μg/mL) and collagen (9.01 ± 0.15 mg/mL) were well retained as compared to the fresh membrane. Notably, the sulfated glycosaminoglycan content of the processed grafts was well conserved (there was only a 21.14% reduction, which was substantially lower than the reduction achieved by conventionally used surfactants for processing biological tissues). The regenerative efficacy of these bioactive scaffolds was evaluated through preclinical testing in a diabetic rodent wound model. It showed a 50% reduction in time to heal compared to the standard of care dressings, supported by increased vascular endothelial growth factor (VEGF) expression in the healed tissues. This can be collectively attributed to the conservation of sulfated glycosaminoglycans (GAGs) and the enhanced scaffold tensile quality, which play key roles in promoting angiogenesis, and tissue regeneration in diabetic wound beds. As a result, these grafts are well suited for a variety of soft tissue reconstruction applications and can also serve as bioactive scaffolds for culturing autologous cells, making them versatile tools in regenerative medicine. 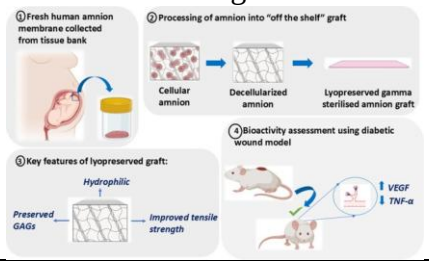
47.	Manifestations of love of sport in Indian elite athletes: An autobiographical study **S Jha, A Amritesh, P Singh** - The International Journal of Sport and Society, 2025 **Abstract:** This research explores the socio-psychological mechanisms and identifies certain aspects of behavioral manifestations of the love of sport from an athlete's perspective. For this study, seven autobiographies of elite athletes from both Olympic and non-Olympic sports were chosen. Reflexive thematic analysis was employed for data analysis. Data was coded through an interactive process to allow common themes to emerge around athletes' love of sports. Four key themes emerged: "striving for excellence," "multifaceted bonding," "primacy of intrinsic rewards," and "peremptory rectitude." The findings demonstrate how "athlete sport love" can be a basis for an athlete's intrinsic motivation for sport as expressed through the identified themes. The findings can assist organizations and policymakers in talent identification and development, athletes' mental health and burnout monitoring, and sports integrity management. The findings critically reflect on earlier conceptions of sport love and extend theories of love into sports by revealing thematic concentrations on certain behavioral aspects unique to sports.
48.	Mitigation of incident wave load on a floating bridge in the existence of horizontal thin porous plate **S Choudhary, SC Martha** - International Journal of Advances in Engineering Sciences and Applied Mathematics, 2025 **Abstract:** The construction of breakwaters can be effectively modelled by using thin porous plates. Therefore, an investigation has been performed concerning the interaction of oblique wave with a floating bridge in the existence of a thin floating horizontal porous plate over an arbitrary bottom. In the present study, Darcy's law simulates the flow via porous structures and Havelock's expansions are used to define the potentials in each region for the mathematical formulation of the physical model. The benefits of the existence of a thin barrier and bottom topography are examined by using several numerical results for wave load acting on the bridge.

	Significant differences in vertical and horizontal forces can be seen between the cases with and without the thin horizontal porous plate and bottom topography. The maximum energy loss corresponds to the minimum in the loads (vertical or horizontal) on the floating bridge. For 55∘≤θ1<90∘ with fixed values of other parameters, both Fv and Fh decrease monotonically for all length and wave frequency values. It is important to highlight from the present findings that the installation of an asymmetric trench and a horizontal porous plate decreases the load on the floating bridge. This may help marine and coastal engineers to design an effective breakwater involving a trench-type bottom and horizontal porous plate.
49.	Modeling, analysis, and online detection of interturn short-circuit fault in medium-frequency transformer of dual-active-bridge converter **TJ Nistane**, S Singh, **S Payami, K Jayaraman** - IEEE Transactions on Industrial Electronics, 2025 **Abstract:** The strident working condition of the dual-active-bridge (DAB) converter has elevated the risk of interturn short-circuit fault (ITTSCF) in medium-frequency transformer (MFT). Thus, it is crucial to analyze the DAB converter under ITTSCF in MFT to avoid the complete winding short-circuit due to insulation failure. Thus, the presented work analyses the variations in the magnetizing and leakage inductance of MFT ranging from low to high severity levels of ITTSCF. Thereafter, its impact on the current stress, power transfer, and zero-voltage-switching (ZVS) of the DAB converter is presented in detail. Based on the analysis, this article presents a new reliable online ITTSCF detection technique for MFT in a DAB converter. This technique utilizes the root-mean-square (RMS) and average-based fault indices generated from the magnetizing current of MFT. The proposed fault detection technique is effective even at low severity ITTSCF (i.e., as low as 1% ITTSCF) and utilizes an off-the-shelf magnetizing current sensor to avoid extra cost. The proposed fault detection technique is immune to load variation and major switch faults in the DAB converter and thereby increases the reliability. For validation, the MFT is designed with winding taps and integrated with the hardware prototype of the DAB converter.
50.	Modulation of H_2 adsorption in C_9N_4 monolayer via biaxial strain for hydrogen storage **P Beniwal, TJ Dhilip Kumar** - Applied Surface Science, 2025 **Abstract:** Two-dimensional (2D) carbon nitride materials hold significant potential as hydrogen storage mediums owing to remarkable chemical stability and large surface area. Prompted by this exploration, leveraging first-principles computations, the hydrogen storage possibility of an innovative C_9N_4 monolayer is studied systematically. H_2 adsorption energy on pristine C_9N_4 lies below the threshold value of −0.20 eV due to weak van der Waals interactions. To optimize the adsorption interaction between the H_2 and monolayer, we explored the hydrogen storage possibilities of a C_9N_4 monolayer when subjected to biaxial strain. The introduction of compressive strain enhanced the reactivity of the monolayer, subsequently improving its adsorption energies. Inducing 4% biaxial compressive strain on C_9N_4, i.e. in 4%ε-C_9N_4, the adsorption energy successfully enhanced and the system adsorbs a single H_2 molecule with −0.32 eV. 4%ε-C_9N_4 monolayer effectively adsorb 8 H_2 molecules, demonstrating the adsorption energy spanning from −0.20 to −0.32 eV, thereby achieving a storage capacity of 8.95 wt%. This work present an effective approach for optimizing the storage attributes of 2D carbon nitrides, serving as an impetus toward the ongoing improvement of advanced hydrogen storage materials. 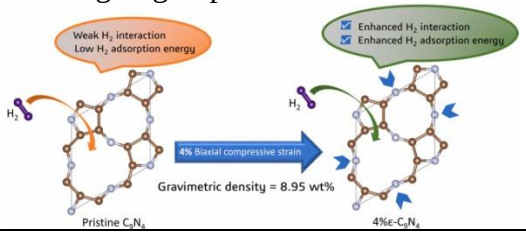
51.	Modulation-assisted drilling of Inconel-718: Multi-variable optimization using response surface

	method **M Singh**, S Dhiman, S Chaudhary, **V Ghai, H Singh** - Journal of Materials Engineering and Performance, 2025 **Abstract:** The effectiveness of film cooling in inconel-718 turbine blades and compressor vanes is primarily regulated by the quality of small holes (< 5 mm) drilled on its periphery. However, as a difficult-to-machine material, the quality of these holes in terms of surface roughness is often compromised when processed using conventional drilling, leading to ineffective cooling and ultimately reducing its service life. In the present study, we have demonstrated the capability of relatively new and sustainable modulation-assisted drilling (MAD) technology to drill superior quality holes in inconel-718. This was achieved by multi-variable optimization of the process parameters, i.e., drill tool diameter (DD), feed rate (FR), and spindle speed (SS), using the response surface method. For this, low-frequency vibrations (frequency, $f_m < 1000$ Hz and amplitude, $2A < 150$ µm) were superimposed on the drill tool using the Tribo-MAM® tool holder (patented device of M4 Sciences) during the drilling experiments. The optimal window was obtained by comparing three decisive output factors–drill tool wear, generated thrust force, and the surface roughness of the holes, investigated over a range of input parameters, i.e., DD (1.5, 2.0, 2.5, 3, and 3.5 mm), FR (0.0035, 0.0095, 0.0155, 0.0215, and 0.0275 mm/rev), and SS (2000, 2200, 2400, 2600, and 2800 rpm). In addition, conventional drilling was also performed at the same set of machining parameters to compare the efficacy of MAD. The obtained results showed the reduction of tool wear, thrust force, and surface roughness by 36, 18, and 49%, respectively, during MAD in comparison to its conventional counterpart. This improvement is primarily attributed to the discrete cutting mechanism resulting from the periodic disruption of tool-workpiece contact. This enhances lubrication, thereby facilitating the efficient removal of discrete chips and contributing to a desired lower surface roughness. The overall superior performance of MAD presented in the current study encourages its widespread industrial use towards precision and sustainable manufacturing.
52.	Multifaceted skeletal effects of Sevelamer carbonate in a secondary hyperparathyroidism model S Sharma, **S Kumar**… **N Kumar**, N Chattopadhyay - Endocrine, 2025 **Abstract:** Introduction: Hyperphosphatemia leads to abnormal mineralization of bones and soft tissues in patients with chronic kidney disease-induced secondary hyperparathyroidism (CKD-SHPT). Sevelamer lowers phosphate levels by binding to dietary phosphate in the gastrointestinal system, forming new bone and reducing the risk of renal osteodystrophy and fracture. However, the influence of sevelamer carbonate (SevC) on bone microarchitecture, material qualities, and mechanical behavior is unknown in CKD-SHPT conditions. Material and methods: We utilized a rat model of CKD-induced hyperphosphatemia by feeding a 1.8% high-phosphate diet to 5/6 nephrectomized rats to test the effects of SevC on skeletal quality and strength, employing microCT, Fourier transform infrared spectroscopy (FTIR), 3-point bending, nanoindentation, and compression tests. Results: SevC preserved mineral homeostasis and reduced PTH, and FGF-23 levels in CKD-SHPT rats. SevC mitigated the serum renal parameters, pyrophosphate levels, and indole acetic acid. In CKD-SHPT rats, SevC reduced hyperphosphatemia, improved the mineralization defect, and upregulated mineralization-promoting genes like ankyrin-1, ectonucleotide-pyrophosphatase/phosphodiesterase-1, tissue non-specific alkaline phosphatase, phosphate-regulating endopeptidase X-linked, dentin matrix protein-1, and matrix extracellular phosphoglycoprotein. In the cortical bones of CKD-SHPT rats, SevC increased cortical mass and thickness, decreased porosity by likely decreasing cortical bone remodeling induced by high PTH, and increased osteocyte preservation. SevC mitigated all of the alterations in the mineral and matrix composition of CKD-SHPT rats, including decreased collagen-maturity, mineral-to-matrix ratio, and increased carbonate substitution of hydroxyapatite crystals. SevC enhanced bone strength and mechanical behavior in CKD-SHPT rats at a macro (three-point bending) and nano (nanoindentation) scales. Conclusion: These findings in CKD-SHPT rats suggest that SevC

	improves bone mechanical properties at various levels by decreasing serum pyrophosphate, empty lacunae, and enhancing renal clearance of indole acetic acid, organized mineral-matrix deposition, and osteocyte number by suppressing cortical remodeling.
53.	Non-modal linear stability analysis of reactive front $A+B\rightarrow C$ for infinitely fast chemical reactions **P Verma**, TK Hota, **M Mishra** - Proceedings of the Royal Society A: Mathematical, Engineering and Physical Sciences, 2025 **Abstract:** A theoretical analysis of viscous fingering instability for a reactive system $A+B\rightarrow C$A+B→C with an infinitely fast reaction in a porous medium for a rectilinear flow is presented. By contrast to the traditional quasi-steady-state analysis (QSSA), a non-modal analysis (NMA) based on the fundamental matrix formulation is employed to study the reactive displacement, considering reactants and products with mismatched viscosities. This study investigates the transient growth of perturbations by analysing the singular values and singular vectors to address the optimal energy amplification. We illustrate that an increase in the viscosity contrast, $\lvert Rb-Rc\rvert$‖Rb−Rc|, resulting from a chemical reaction for a given endpoint viscosity contrast RbRb, leads to a more unstable system. However, there exist some reactions when $Rc>Rb$Rc>Rb, the onset delays than the equivalent non-reactive case, $Rc=Rb$Rc=Rb. It suggests that the stability of the flow is primarily influenced when instability develops downstream within the flow. Furthermore, RbRb is found to significantly affect the spatio-temporal evolution of perturbations and the underlying physical mechanism. It is demonstrated that the QSSA is inadequate to address the transient growth, and NMA is the most suitable approach to studying the underlying physical mechanism of instability. Furthermore, NMA results align more consistently with non-linear simulations compared with QSSA.
54.	Non-Newtonian fluid droplet impact dynamics on thin liquid films **M Singh**, S Basu, **D Samanta** - Physics of Fluids, 2025 **Abstract:** Droplet impact on liquid films is a ubiquitous phenomenon in nature and many industrial applications. The present study highlights the impact dynamics of viscoelastic droplets on thin films of water and the same viscoelastic fluid as the droplet. In this experimental study, we have highlighted the variations in the impact dynamics that arise due to the non-Newtonian effects. The ejection of secondary droplets from the crown rim normally observed in the case of Newtonian droplet impacts on water films is suppressed, in the case of non-Newtonian droplet impacts on water films. Due to the fluid elasticity, the Rayleigh–Plateau instability-induced ejection of secondary droplets from the crown rim is inhibited. Long-lasting slender liquid filaments resembling beads-on-a-string structures are observed in the case of viscoelastic droplet impact on water films. However, when the drop and film are of the same viscoelastic fluid, such filaments are not observed during the crown formation stage. Subsequently, we have characterized the geometrical features of the crown and the regime maps of various outcomes of the droplet impact dynamics. It is observed that the elasticity of the liquid suppresses the crown growth and secondary droplet formation. The dependence of the impact dynamics on Weber number (We), polymer concentration in terms of elasticity number (El), Bond number (Bo), and film thickness (h*) are also highlighted in the form of regime maps. It is observed that secondary droplet ejection does not take place on an increase in Bond number and film thickness for both water and viscoelastic films.
55.	Novel PEGylated deep eutectic solvents: A thermophysical and photophysical investigation Y Vora, **M Prajapati**…**Kumar**, S Pandey, K Kuperkar - Journal of Molecular Liquids, 2025 **Abstract:** Deep eutectic solvents (DESs) have gained significant interest among researchers in the past two decades due to their improved physical and chemical characteristics beyond traditional organic solvents. They represent a recent advancement in eco-friendly solvents.

	Studying their physical characteristics would thus be very beneficial for designing methods in varied application domains. A majority of DESs are traditionally categorized into several types. Amongst them, the recently known Type V DESs have received increased attention. They are made using nonionic precursors that frequently exhibit marginal high vapor pressure and lower viscosities than their ionic equivalents and are chloride-free. In this study, four new PEGylated DESs are successfully prepared by using polyethylene glycol 200 (PEG200) as a hydrogen bond donor (HBD) with varied organic acids such as levulinic acid (LA), cinnamic acid (CIA), hydrocinnamic acid (HCA), and citric acid (CA) as hydrogen bond acceptor (HBA) in different molar ratios. Various atomic interactions between the HBAs and HBD in these prepared DESs were explained using Fourier transform infrared (FT-IR) spectroscopy and ^{1}H- and ^{13}C-nuclear magnetic resonance (^{1}H- and ^{13}C NMR) spectroscopy. Also, the temperature-induced transition in the prepared DESs was recorded using differential scanning calorimetry (DSC) and thermogravimetric analysis (TGA). The thermophysical properties, such as density (ρ) and viscosity (η), were defined as a function of temperature. Also, the study investigates the physical and chemical properties of PEGylated DESs, focusing on their dipolarity/ polarizability, solvatochromic behavior, chemical structure, and composition. It uses Kamlet-Taft parameters to explore the H-bond donor and acceptor tendency and understand the role of acidic constituents. The study also investigates the solvation dynamics and diffusion of fluorescence quenching of pyrene and benzo [a]pyrene using nitromethane as a quencher. Here, the fluorescence lifetime adheres to the Stern–Volmer fitting, and higher bimolecular quenching rate constants support the faster diffusion of fluorophore and quencher molecules in these PEGylated DESs compared to other hydrophilic DESs. The study establishes constituent dependence and faster solvation dynamics. 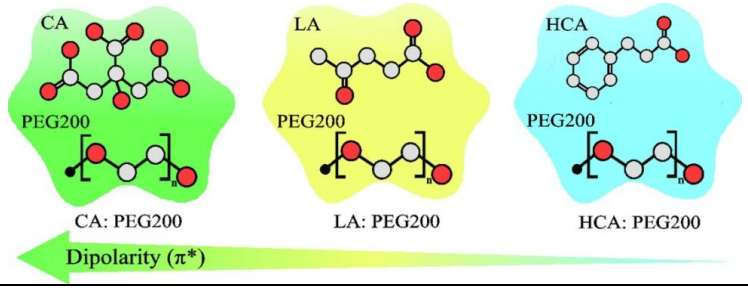
56.	Optimal allocation of multiple rigid bars with unequal draft to enhance Bragg reflection of surface gravity waves **D Goyal, SC Martha** - Ships and Offshore Structures, 2025 **Abstract:** Bragg resonant reflection is a widely acknowledged phenomenon that can occur when a sequence of submerged artificial bars are equidistantly positioned along the littoral of the coastal zone, provided that the wavelength of the incoming wave train is about twice the distance between the bars. In order to optimise the sustainability of breakwaters by preventing multiple zero reflections and enhancing Bragg reflection, the current study investigates the most advantageous placement of a series of rectangular bars in close proximity to coastlines. Four different types of the series allocation are examined, such as (a) a series of bars arranged in a pattern that resembles a Gaussian pattern, (b) a series of bars arranged in a pattern resembling a parabolic opening, (c) a series of bars arranged in monotonically decreasing positions, and (d) a series of bars arranged in a monotonically increasing position. The bars are equally spaced and do not have the same height (i.e. submergence depth). The computationally feasible boundary element method is employed to solve the boundary value problem. The physical entities namely, the reflection and transmission coefficients on the multiple structures are calculated to check the efficiency of the optimal allocation of the multiple bars. The outcomes of this study demonstrate that the systematic arrangement of rectangular bars in a monotonically declining or ascending pattern, as opposed to maintaining a constant level, effectively removes zero reflections and enhances the intensity of resonant peaks and effective bandwidth. One notable benefit is that

	engineers can enhance the effectiveness of a Bragg breakwater by strategically stacking several bars in an ideal allocation, all while maintaining the same capital expenditure and resources.
57.	Optimizing pine needle pyrolysis: The role of pre-treatment in boosting bio-oil quality for sustainable energy production **A Jaswal, R Goswami, PP Singh, T Mondal** - Biomass Conversion and Biorefinery, 2025 **Abstract:** This study investigates the transformative potential of pre-treatment methods on the pyrolysis of pine needles, a plentiful forestry residue in Uttarakhand, India. The work focuses on how various pre-treatment strategies—chemical treatments using dilute acid (5 wt.%) and alkali (5 wt.%) solutions, as well as thermal torrefaction—affect biomass properties, the pyrolysis process, and the quality of the resulting bio-oil. Characterization of pre-treated samples revealed substantial changes compared to untreated pine needles. Proximate analysis indicated significant reductions in ash content, with the most considerable decrease observed in acid-treated samples. Additionally, there were notable reductions in volatile matter and moisture content, while fixed carbon content increased across all treatments, particularly in torrefied samples. Ultimate analysis demonstrated an increase in carbon content and a reduction in oxygen content for acid-treated and torrefied samples, whereas alkali treatment exhibited the opposite trend. Alkali treatment led to the highest mass loss (50%) due to extensive lignin and hemicellulose removal while torrefaction led to the lowest mass loss (20%). When evaluating the pyrolysis of pre-treated samples under these optimized conditions, significant changes in product distribution were observed. Acid treatment enhanced bio-oil yield to 46.5%, whereas alkali and torrefaction reduced yields to 30% and 35.5%, respectively. Notably, torrefaction yielded the highest quality bio-oil with the highest phenolics content, an HHV value of 25 MJ/kg and the lowest water content (21.5%), highlighting its efficacy as a pre-treatment method for improving energy production from biomass. By understanding how different pre-treatment strategies affect biomass properties and pyrolysis processes, this work paves the way for more efficient, cost-effective biomass valorization, promoting the use of pine needles as a viable, renewable feedstock for biofuel production.
58.	Outage analysis of downlink RSMA in vehicular cluster: A copula-based approach **S Bhattacharyya, S Darshi**, Z Lin - IEEE Wireless Communications Letters, 2025 **Abstract:** The surge in on-road vehicles is fueling the need for the adoption of technologies like rate-splitting multiple access (RSMA) to meet the demand for higher data rates and enhanced quality-of-service (QoS). However, a key challenge in RSMA lies in addressing the inherent dependency between the common and private streams, which complicates outage analysis. This dependency arises not only due to interference between the streams but also from the necessity of decoding both streams for successful reception. Accurately modelling this dependency is crucial, yet it remains largely unexplored. This letter introduces a novel copula-based framework to model the dependency in downlink RSMA for vehicular clusters, where maximal ratio transmission (MRT) is used for the common stream and zero-forcing scale-down (ZF-SD) for the private streams. By deriving the analytical outage probability expressions and validating them with Monte Carlo simulations, we provide a comprehensive performance analysis. Additionally, we explore the impact of power allocation on both outage and throughput, offering practical design insights for RSMA-enabled vehicular systems.
59.	Performance analysis of solar collector integrated with porous metallic foam **V Kulkarni, AS Kashyap**, M Pal, **H Tyagi** - Applied Sciences, 2025 **Abstract:** The use of solar energy is a promising solution to reduce dependence on fossil fuels. Flat-plate collectors (FPCs) are commonly employed to harness solar energy, but their performance is often limited by thermal resistance, surface deterioration, and inefficient heat dissipation. This study investigates the performance enhancement of an FPC integrated with porous copper foam through numerical simulations. The porous foam increases surface area and

	improves heat transfer by creating a complex flow path for the working fluid. Key parameters such as the porous foam height ratio (S), Darcy number (Da), and volumetric flow rate ($\dot{V}$) are analysed to determine their impact on thermal performance. The results indicate that a maximum Nusselt number (Nu) of 28.85 and an outlet temperature of 306.81 K is obtained for S = 1. A decrease in Da from 10^{-2} to 10^{-6} and an increase in $\dot{V}$ from 0.25 L/min to 1 L/min enhance the Nu by 5.7% and 8.8%, respectively. The friction factor (f) increases with increases in S, a decrease in Da and an increase in $\dot{V}$. The performance evaluation criteria (PEC) are obtained to be maximum at S = 0.4, Da = 10^{-2} and $\dot{V}$ = 0.25 L/min. These findings demonstrate the potential of porous copper foam in improving FPC efficiency.
60.	Photocatalytic hydrogenation of levulinic acid and furfural to fuel additives over RU-decorated carbon-channelized catalyst **A Chauhan, R Ghalta, R Srivastava** - ACS Sustainable Chemistry & Engineering, 2025 **Abstract:** γ-Valerolactone (GVL) and cyclopentanol (CPL) are valuable biomass-derived chemicals with applications as green solvents, renewable fuels, and intermediates in polymers and pharmaceuticals. However, their conventional synthesis requires high energy and expensive catalysts. Here, we report a Ru-decorated g-C_3N_4 (CN) and phytic acid-derived carbon (CP) composite (Ru@CP1/CN1) as an efficient photocatalyst for the selective transformation of levulinic acid (LA) to GVL and furfural (FUR) to CPL under mild conditions with simultaneous water splitting. The Ru@CP1/CN1 catalyst achieves ∼99% selectivity for GVL in 6 h and 86% selectivity for CPL in 9 h with nearly complete conversion. The superior performance is attributed to enhanced charge separation, facilitated by the CP support, enabling efficient electron transfer from CN to Ru active sites. In situ X-ray photoelectron spectroscopy (XPS) and ultraviolet photoelectron spectroscopy (UPS) confirm the charge transfer mechanism, while control experiments, deuterium labeling, in situ IR spectroscopy, and EPR analysis provide mechanistic insights. The catalyst demonstrates excellent stability, maintaining activity and selectivity over five consecutive cycles. This work establishes Ru@CP1/CN1 as a promising photocatalyst for sustainable biomass valorization, offering an energy-efficient and selective pathway for green chemical production and fuel additives. 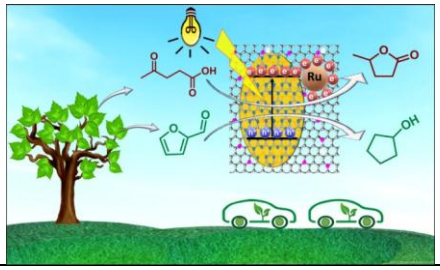
61.	Photothermal analysis of novel nanoparticles-laden fluid-based solar thermal receiver: A proof-of-concept experimental study **JSD Nandini**, V Bhalla, **H Tyagi** - International Journal of Thermofluids, 2025 **Abstract:** Excessive extraction of fossil fuels leads to air pollution, water pollution, destruction of habitat, etc., which are some of the severe environmental consequences. Directing towards renewable energy sources like solar and wind energy helps to attenuate these impacts and promote a purified, healthier environment for future generations. Solar energy is infinitely available and used for present and future energy needs. Thus, by utilizing this power, we can mitigate the carbon footprint, greenhouse gas (GHG) emissions, etc., which helps to build a secure, clean energy future. This experimental study compared the photo-thermal effects of surface absorption and nanoparticle-laden systems on the moving flow characteristics of the nanoparticle-laden fluid in a novel spiral solar collector. The influence of channel depth (10 and 20 mm) and volume flow rate on temperature rise has been investigated in this experimental investigation, and it has been discovered that the nanoparticle mass fraction (optimum mass

	fraction of the nanoparticles) relies on channel depth. Experimental results show that for optical depth of 10 mm, a temperature rise of 11.4°C is obtained at the optimum mass fraction of 40 mg/L, and compared to this, at the optical depth of 20 mm, a temperature rise of 6.7°C has been achieved at the optimum mass fraction of 10 mg/L. After evaluating the influence of volume flow rate (25–200 mL/hr), a maximum temperature rise of 11.2°C was obtained at 25 mL/hr. In all cases, the temperature rise in the N-VAS (Nanoparticle-laden volumetric absorption-based system) is more significant than S-BAS (Surface-based absorption system), indicating that the presence of nanoparticles results in a higher heat transfer rate by absorbing more radiation from the heat source. 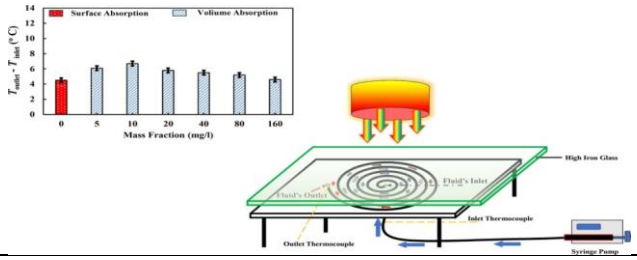
62.	Potential applications of elastic instability and elastic turbulence: A comprehensive review, limitations, and future directions **C Sasmal** - Journal of Non-Newtonian Fluid Mechanics, 2025 **Abstract:** Viscoelastic fluids, a subclass of complex fluids, are employed across various applications, from biological processes to large-scale industrial operations. These fluids exhibit complex flow behaviors resulting from non-linear elastic stresses that arise from the stretching and relaxation of their microstructures, such as polymer molecules in viscoelastic polymer solutions, within a deformed flow field. One notable phenomenon associated with these fluids is purely "elastic instability" (EI), which occurs when elastic stresses interact with the streamline curvature in a flow system at low Reynolds numbers (the ratio of inertial to viscous forces). Specifically, EI manifests when the Weissenberg number (the ratio of the microstructure relaxation time to the rate of flow deformation) surpasses a critical threshold. As the Weissenberg number continues to increase, the unstable flow field resulting from EI further transits to a more chaotic and turbulent-like flow state known as "elastic turbulence" (ET). The fluctuating hydrodynamics characteristics of ET display statistical similarities to conventional Newtonian turbulence observed at high Reynolds numbers. Over the past two decades or so, extensive research has been conducted within the complex fluids research community to explore these two phenomena, resulting in several comprehensive articles that outline the development and understanding of ET. This article focuses on the potential application perspectives of these two phenomena. In particular, this article aims to provide a thorough review of the applications of EI and ET phenomena, particularly in three main areas: microfluidic mixing, microscale heat transfer, and chemically enhanced oil recovery (EOR) processes. Furthermore, this review will also provide a discussion on the limitations and future research directions associated with these two phenomena, highlighting their potential from an application standpoint.
63.	Purcell enhanced laser action using a super-Tamm cavity mode SM Lis S… **FH Lone, N Singh**, D Banerjee, **RV Nair**, S Bhaktha BN - Optics Letters, 2025 **Abstract:** Optical Tamm structures have potential for the development of optoelectronic devices, provided they overcome the challenge of low-quality factor of modes and inherent losses associated with plasmonic metal films. In this work, we present lasing in a super-Tamm structure consisting of a silver thin film deposited on a 4-(dicyanomethylene)- 2-methyl-6-(4-dimethylaminostyryl)-H-pyran (DCM) dyedoped polyvinyl alcohol (PVA) spacer layer coated on a SiO2 /TiO2 one-dimensional photonic crystal with a lasing threshold of ~0.07 mJ. The spectral line narrowing and threshold characteristics observed in the emission spectrum corroborate the realization of a waveguided super-Tamm laser. The bi-exponential temporal decay profile of the

	Tamm lasing modes with an average lifetime of 0.52±0.02 ns confirms the Purcell enhancement of radiative intensity of the DCM dye when coupled to the super-Tamm modes.
64.	Rapid detection and visible light driven photocatalytic degradation of chloramphenicol in aqueous medium using a CoAl2O4/rGO nanocomposite **K Kaur, T Akhtar**, G Singh, N Kaur, **N Singh** - New Journal of Chemistry, 2025 **Abstract:** Nanoscale materials employed in the electrochemical detection of chloramphenicol (CAP) have attracted significant research attention due to concerns regarding antibiotic residue detection in water and food products, associated with widespread contamination of water reservoirs by human and veterinary waste. Graphene-based materials are especially intriguing because of their π–π interactions. In the present work, $CoAl_2O_4$ and reduced graphene oxide (rGO) have been used to modify glassy carbon electrodes (GCEs). The synthesized $CoAl_2O_4$/rGO nanocomposite was characterized through various techniques such as XPS, FE-SEM, EDS, Raman spectroscopy, FTIR, and HR-TEM. The electrochemical performance of $CoAl_2O_4$/rGO for CAP determination was evaluated using cyclic voltammetry (CV), differential pulse voltammetry (DPV), linear sweep voltammetry, and chronoamperometry techniques. The $CoAl_2O_4$/rGO exhibited linear detection limit = 13.5 nM, limit of quantification = 19.34 nM, and sensitivity = 1.1505 μA μM^{-1} cm^{-2} with a linear calibration equation of I_{pc} (μA) = 0.3895[CAP]/(μM) + 0.1599 having R^2 = 0.9957. Additionally, $CoAl_2O_4$/rGO showed excellent selectivity and anti-interference towards CAP recognition. The $CoAl_2O_4$/rGO showed promising potential for CAP analysis in tap water, river water, and pharmaceutical wastewater with good % recovery rates. Moreover, the $CoAl_2O_4$/rGO nanocomposite is an efficient catalyst for the photodegradation of CAP as revealed by the UV-vis spectroscopy results, which showed that the $CoAl_2O_4$/rGO nanocomposite exhibits 100% CAP degradation efficiency within 80 min under natural sunlight and displays good stability and reusability of the catalyst. 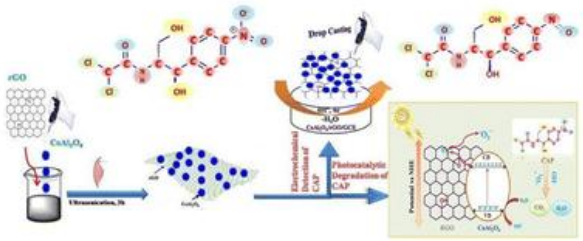
65.	Seismic behaviour of timber-reinforced masonry housing typologies in the Himalayan Region: A state-of-the-art survey PKVR Padalu, **M Surana, AS Rajput** - Iranian Journal of Science and Technology, Transactions of Civil Engineering, 2025 **Abstract:** In the Himalayan region, traditional buildings made of masonry have existed for centuries and still make up a sizable portion of the building stock. Many of these buildings have proven records of earthquake resilience. At the same time, the primary cause of fatalities from previous earthquakes is the increasing collapse of unreinforced masonry structures. In various Himalayan locations, local seismic culture has evolved over the past few centuries to improve the seismic capacity of stone constructions. These areas use wood or other materials with high tensile strength to reinforce their stone masonry. The post-earthquake reconnaissance surveys clearly demonstrate the superior performance of these timber-reinforced masonry constructions. Nevertheless, there is still a lack of scientific investigation, either through numerical modelling or laboratory-based studies, on the behaviour and mechanism of these structures. Furthermore, there are no explicit criteria for evaluating timber-reinforced masonry in the present Indian seismic code. This study examines several distinct traditional masonry building typologies found in the Himalayas, such as ‘Thathara’, ‘Kath-Kuni’ or ‘Koti-Banal’, ‘Newari’, ‘Dhajji Dewari’, ‘Ikra’ or ‘Assam-Type House’, ‘Bhatar’ or ‘Taq’, and ‘Dry-stone buildings’. For the majority of these

	typologies, aside from Dry-stone houses, the masonry walls have embedded horizontal timber bands or lacings that enhance box behaviour, thereby preventing premature failure. Through a thorough analysis of timber-reinforced masonry, including architectural details, earthquake-resilient & vulnerable features, and experimental and numerical investigations, the article presents a unique addition to our understanding of seismic performance and how it might best protect the Himalayan region's traditional heritage. Additionally, the current study contributes to a better understanding of how wood elements give masonry structures greater seismic resilience. This understanding will help with several initiatives: (i) better conservation, preservation, and maintenance of traditional or heritage structures; (ii) seismic codes/standards providing details regarding the assessment of timber-reinforced structures; (iii) supporting and encouraging practitioners to design and build using techniques that have demonstrated superior performance, and (iv) as attempts to lessen the impact of building on our environment increases, provide a way to make safer structures utilizing low-carbon materials.
66.	Supporting mental health: pre-post four-week psychological capacity building program for Indian target sport athletes **S Gill, P Singh** - Human Movement, 2024 **Abstract:** Purpose: Mental training, widely recognised in sports psychology, has not been fully utilised to address broader mental health concerns among athletes, especially in India. This study examines the Psychological Capacity Building Program (PCB P) for Indian shooters and archers, focusing on key psychological variables such as motivation, grit, emotions, and well-being. The four-phase program includes sports analyses, individual assessments, motivational tasks, a one-week psychoeducational phase on mental skills, and two weeks of applying these skills in the athlete's daily training routines. Methods: Psychometric tools such as the Sports Motivation Scale-II (SMS-II), Mental Health Continuum-Short Form (MHC-SF), Sports Emotion Questionnaire (SEQ), and Grit Scale were used to measure pre- and post-intervention scores of 122 athletes, divided into experimental (n = 60) and control (n = 62) groups. Within-group and between-group analyses were conducted, along with effect size calculations. Results: The experimental group showed significant improvements in happiness ($p < 0.001$), emotional well-being ($p = 0.017$), intrinsic motivation ($p = 0.006$), and grit ($p = 0.004$), alongside reductions in dejection ($p = 0.001$) and non-regulation ($p < 0.001$). In contrast, the control group experienced increased anger ($p = 0.005$) but no other significant changes. Between-group comparisons revealed greater reductions in anxiety ($p < 0.001$) and significant improvements in happiness ($p < 0.001$), emotional well-being ($p < 0.001$), social well-being ($p < 0.001$), and grit ($p = 0.004$) in the experimental group. Conclusions: PCB P shows promise for enhancing the athlete's mental health, but further research with larger samples is needed to confirm its effectiveness and long-term adaptability across diverse sports.
67.	Synergistic effect of MoS2 and Ag on high-temperature Tribology of self-lubricating Ni-based composite coatings by cold spray deposition RKS Gautam… **H Nautiyal**, R Kumar - Journal of Thermal Spray Technology, 2025 **Abstract:** As technology advances, tribo-coupling components, viz. gears, seals, bearings etc., frequently function under severe conditions, and this enhanced the demand of effective lubrication for reduced friction and wear of contacting interfaces. The optimal content of solid lubricants in the matrix is a viable alternative to acquire the desired lubrication in extended regime of temperatures. The present work investigates the tribological characteristics of cold sprayed Ni-based self-lubricating composite coatings with varying content of Ag (5, 10, 12.5 and 15 wt.%) and fixed concentration of MoS_2 (10 wt.%). The mechanical, microstructural and the tribological properties were evaluated from room temperature (RT) to 800 °C. The results revealed that the coating having 12.5 wt.% of Ag along with 10 wt.% of MoS_2 has delivered superior lubricity among all compositions in terms of lower coefficient of friction COF (0.18) and wear rate 5×10^{-5} mm^3/Nm at 800 °C. The average COF, without the use of Ag and MoS_2,

	has attained (0.49) at 800 °C. However, the coating containing 12.5 wt.% of Ag has attained increased COF (0.38) and wear rate 7.1×10^{-5} mm^3/Nm at 400 °C; thereafter, a declining trend was observed. The improved frictional properties were accredited to the synergistic effects of impregnated solid lubricants and novel lubricious phases (Ag_2MoO_4, $Ag_2Mo_2O_7$, $Ag_2Mo_4O_{13}$ NiO, etc.) formed on the worn surface. The observed wear mechanisms were correlated with the morphologies and tribo-chemical reaction between the contacting interfaces.
68.	Tackling impurities in CCS pipelines: An optimization-based approach **MM Laljee**, A AlHajaj - Case Studies in Chemical and Environmental Engineering, 2025 **Abstract:** Carbon capture and storage (CCS) is crucial for carbon neutrality, requiring efficient CO_2 transport through pipelines. This study introduces an efficient optimization-based model for designing cost-optimal pipelines with a compressor-pump assembly and intermediate boosters, considering impurities such as Argon, Methane, hydrogen and Nitrogen, which impact stream density, pressure drop, and levelized transport costs (LCOCT). Impurities reduce throughput by 3.6 % and increase compression energy by 11 % (from 100.11 to 111.14 kWh/ton CO_2), accounting for 30 % of CCS equivalent energy. A penalty scheme (e.g., US'84/ton CO_2 for 4 % N_2) offsets impurity costs, highlighting the need for impurity control in efficient CCS deployment.
69.	Tailored fibrils approach via Ag(I). Peptidomimetic-based interface design: Efficient encapsulation of diverse active pharmaceutical ingredients in wastewater remediation during effluent treatment plant (ETP) processing **A Sharma**, N Kaur, **N Singh** - Langmuir, 2025 **Abstract:** Pharmaceutical pollution in wastewater poses significant environmental and public health concerns worldwide. Chloramphenicol (CP), an antibiotic widely used in medical and veterinary applications, is among the active pharmaceutical ingredients (APIs) frequently detected in aquatic environments. This study explored the encapsulation of chloramphenicol API in contaminated wastewater using rationally designed fibrations based on the silver metal ion-directed self-assembly of fibrillator-type self-assembling ligand (**ANS-3**). We further investigated the removal of various commonly prescribed drugs, including antibiotics such as β-lactam (amoxicillin), fluoroquinolone (ciprofloxacin), aminoglycoside (neomycin), and tetracycline; antiparasitic agents with antiprotozoal properties (praziquantel and metronidazole); nonsteroidal anti-inflammatory drugs (NSAIDs) such as phenylbutazone and ketoprofen; the vasodilator isoxsuprine; amphiphilic antidepressants (amitriptyline); and the antiviral drug amantadine. The findings validated the crucial influence of polar multifunctionality and structural complexity in enhancing interactions with **Ag**.**ANS-3** matrix, emphasizing its potential for efficient drug sequestration. First, picolinic acid (PA) and phenylalanine (F) were evaluated for their ability to form fibrillar structures, and their morphological characterization revealed well-defined fibrillar networks with varying degrees of porosity and interconnectivity. Then, the strategic inclusion of leucine in synthesizing **ANS-3** facilitated the formation of robust fibrillar networks, employing its hydrophobic interactions to drive the self-assembly process. Finally, the encapsulation of APIs was evaluated using Ag(I) metal ion-driven **ANS-3** based self-assembled nanofibrous material. This research contributes to the development of innovative physicochemical wastewater treatment strategies for environmental remediation and validates the importance of rational design in encapsulation-based wastewater remediation technologies. 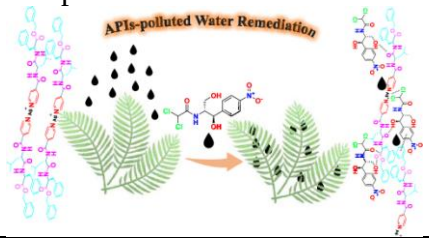

70.	Thermofluidics design evolution of biomimetic micropillar wick for thin-film evaporative cooling **S Anand, CS Sharma** - Bulletin of the American Physical Society, 2024 **Abstract:** Thin-film evaporative cooling in heat pipe and vapor chamber is a promising approach for passive cooling of microelectronics. This study reports the development of a capillary wick design, consisting of an array of wedged micropillars inspired by the peristome of Nepenthes alata. The sharp wedge corners lead to high meniscus curvature. The resulting large capillary pumping pressure, coupled with high permeability of the array, can achieve ~234% higher dryout heat flux compared to the cylindrical micropillar array. However, fabrication of these micropillars using optical lithography and DRIE results in large radius of curvature at the wedge corners, which significantly decreases its thermofluidic performance. We adopt several alternative fabrication approaches to improve the wedge corner sharpness, including the use of serif structures and e-beam lithography. We find that e-beam lithography achieves the requisite wedge geometry. However, upscaling the process to large footprint area is challenging. In view of these challenges, we propose a new design of wedged micropillars that compensates for finite corner radius, can be fabricated using optical lithography and DRIE, and can deliver dry-out heat flux performance equivalent to that of sharp wedge corner micropillars.
71.	THz hybridization in CRAN-based vehicular networks: Performance and handoff implications **SK Singh**, N Gupta, R Singh, **B Kumbhani** - IEEE Communications Letters, 2025 **Abstract:** In this letter, we propose a modified cloud radio access network (CRAN) configuration to enhance vehicular connectivity. The proposed CRAN integrates sub-6 GHz through Macro-Remote Radio Heads (M-RRHs) and terahertz (THz) waves with Terahertz Stations (TSs). Besides, to effectively utilize the potential of THz and sub-6 GHz bands, we consider the two distinct traffic zones (i.e., dense zone and sparse zones). Further, we derive analytical closed-form expressions for coverage probability and hand-off aware rate for both zones to analyze the performance variations across sub-6 GHz and THz frequencies. Through simulations, we demonstrate the effectiveness of the proposed approach compared to baseline approaches.
72.	ToSiM-IoT: Towards a sustainable optimisation of machine learning tasks in internet of things **A Kaushal**, O Almurshed, A Muftah, **N Auluck**, O Rana - IEEE Internet of Things Journal, 2025 **Abstract:** With the rise of digital infrastructure and Internet of Things (IoT), a substantial amount of data is continuously generated that needs to be processed efficiently. While modern artificial intelligence (AI) approaches have shown good capabilities in handling large volumes of data, their excessive demands for memory and processing power result in very high utilisation of resources. In this work, we propose ToSiM-IoT, an optimisation framework that introduces a layer selection approach to identify an ideal mix of active, and inactive layers, using a genetic algorithm for model training. Next, we design a pruning mechanism that identifies performance-critical features using heatmap visualisation, during model inference, and eliminates the remaining features. Two machine learning (ML) models – InceptionV3 and VGG16, have been evaluated on an agricultural weed detection scenario, using the DeepWeeds image classification dataset. Experimental results demonstrate that our framework can achieve a significant reduction in model size and training time, while maintaining high accuracy, for both models. Therefore, this approach provides the potential to be efficiently deployed on intelligent IoT systems where computational capabilities are limited.
73.	Ultrafast, self-powered and highly-stable PtS-Ga_2O_3 heterojunction photodetector for broad-spectrum sensing **D Kaur, R Dahiya, V Sheokand, G Bassi, M Kumar** - Surfaces and Interfaces, 2025 **Abstract:** Noble metal chalcogenides (nMC), special class of 2D non-layered materials, are

	gaining traction due to their exceptional qualities like high carrier mobility and higher active sites at surface. From optoelectronics perspective, their unsaturated dangling bonds lead to higher photoresponse but at expense of prolonged carrier lifetime, thereby making devices slower. Platinum monosulfide (PtS) is one such nMC possessing great potential but currently plagued with slower switching times and stability issues. Herein, we report an ultra-fast and self-powered broadband photodetector of PtS by interfacing with amorphous Ga_2O_3 leading to microsecond response. Heterojunction devices show speeds of 84µs/100µs at self-bias (biasing reduces it further) and are stable even after 7500 h as opposed to bare PtS device, which shows neither. Interfacial band alignment explains working of device, thereby, revealing synergistic combination of nMC with wide-bandgap material, broadening the horizon of nMC-based self-powered optoelectronics. 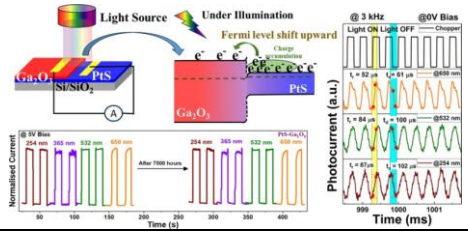
74.	Unveiling critical transition in a transport network model: Stochasticity and early warning signals **SN Chattopadhyay, AK Gupta** - Nonlinear Dynamics, 2025 **Abstract:** Abrupt shifts between stable states frequently occur in complex systems, from natural phenomena like ecosystem collapse to engineered systems namely traffic flow. These transitions, which can be sudden and severe, are anticipated using statistical tools or early warning signals (EWSs), valued for their broad applicability. This study examines a two-dimensional autonomous vehicular traffic flow model and extends it with a stochastic version using a multiplicative Gaussian process. PRCC analysis is conducted to gain an in-depth understanding of the model's robustness and assess how variations in different parameter configurations affect the results. Detailed bifurcation analysis reveals important characteristics of the deterministic model, including bistability, tristability, and tetrastability. Phase portraits and basin stability measures further investigate these bifurcation results. It is revealed that transitions between low-density and high-density traffic regimes can occur due to saddle-node bifurcations and noise. Two-parameter diagrams pinpoint specific domains where the system achieves unique or multiple equilibrium points, illustrating how parameters influence the number of steady states. The confidence ellipse method identifies threshold noise levels signalling a shift between attractors. EWSs are utilised to predict regime shifts caused by bifurcation-induced and noise-driven transitions. In the former, variance serves as a strong predictor, effectively detecting critical shifts due to changes in exit rates, while lag-1 autocorrelation proves less reliable. In the stochastic switching context, lag-1 autocorrelation performs marginally better than variance. Additionally, conditional heteroskedasticity is also employed to detect B-tipping and N-tipping points prior. However, its performance gets hampered while anticipating the second instance. These findings suggest that EWSs can effectively predict critical traffic transitions if applied with caution. The study offers valuable insights for traffic management strategies to anticipate and alleviate congestion in urban networks.
75.	Unveiling magnetic states in nanotubes: Insights from remanent ferromagnetic resonance spectroscopy **A Kumar, C Kalouni, R Posti**, D Tiwari, VK Malik, **D Roy** - Physica Scripta, 2025 **Abstract:** Magnetic nanotubes have garnered immense attention for their potential in high-density magnetic memory, owing to their stable flux closure configuration and fast, reproducible reversal processes. However, characterizing their magnetic configuration through straightforward methodologies remains a challenge in both scope and detail. Here, we elucidate the magnetic

	state details using Remanence Field Ferromagnetic Resonance Spectroscopy (RFMR) for arrays of electrodeposited nanotubes. Micromagnetic simulations revealed distinct spin configurations while coming from saturation, including the edge vortex, onion, uniform and curling states, with chirality variations depending on the preparation field direction. We identified individual spin configurations, as depicted in our micromagnetic simulations, through careful measurements of the RFMR spectra starting from both positive and negative saturation. The Observations revealed opposite RFMR spectra, indicating opposite magnetic spin configurations after removing the positive and negative saturating fields when the magnetic field was applied along (θH=0o) and perpendicular (θH=90o) to the nanotube axis. We observed a mixture of the non-uniform curling states with the end vortex state (onion-like curling state) at the end of the nanotubes for the θH=0o(90o) and uniform magnetization states in the middle of the nanotubes for the θH=0o configuration. Dynamic measurements in presence of the bias field, coupled with RFMR spectra analysis, provided insights into the evolution of individual modes. Additionally, our FMR analysis indicates nucleation within the edge vortex state, which was further corroborated by micromagnetic analysis and substantiated with First Order Reversal Curve (FORC) measurements.
76.	Uranium concentration from acidic mine effluent using forward osmosis **M Verma, VA Loganathan** - Journal of Environmental Management, 2025 **Abstract:** Uranium (U) is found in the earth's crust at concentrations ca. 1 to 3 ppm, which presents opportunities for various industrial and hydrometallurgical processes aimed at achieving economical and low-energy-intensive extraction. In this study, we assessed the potential of forward osmosis (FO) to concentrate the uranium mine effluent using sodium sulphate as draw solution. The diluted draw solution can be directly reused as a raw material in the uranium leaching process without the need for regeneration. Laboratory FO experiments were performed for 160 h duration on synthetic uranium solution representing typical mine effluent characteristics of the Jadguda uranium extraction facility, Bihar, India. The results of the study showed that with forward osmosis, uranium can be concentrated to ca. 3.36 times of its initial concentration and ca. 98% rejection, but with considerable flux decline due to membrane fouling and surface crystallization. Further, the membrane can be operated after regeneration using DI water rinsing or physical cleaning with a lower flux recovery of 83.1% and 81.2%, respectively. Importantly, it was observed that operating membrane below critical concentration factor via cyclic mode can avoid surface crystallization and subsequent membrane fouling with least periodic maintenance. Additionally, with FO concentration process the U concentration much lesser than Indian regulatory guidelines for inland water discharge (i.e. 180µg of U L^{-1}) could be achieved using draw solution. Our study highlights that the FO concentration process can significantly concentrate uranium mine effluent at room temperature, requiring less specific energy compared to conventional evaporation-based processes that are highly energy-intensive. 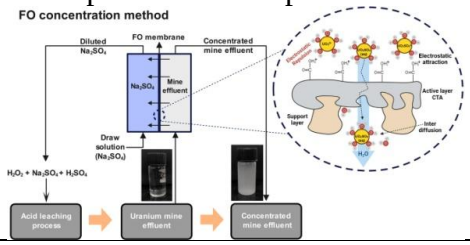
77.	Wiener type theorem for some operator algebras and elements of Banach algebra PA Dabhi, **KB Solanki** - Journal of Mathematical Sciences, 2025 **Abstract:** Weighted p−power analogues of Wiener type theorem are obtained for off-diagonal decay rates of inverses of (infinite) matrices of operators, vector valued functions that are periodic at infinity, operators whose matrix entries are generated using (Parseval) frame, fusion frame, fuzzy fusion frame and g−frame, almost periodic elements of Banach algebras and

	difference operators.
78.	XAI-INVENT: An explainable artificial intelligence based framework for rapid discovery of novel antibiotics R Sharma… **A Kumar**, AK Singh, S Saxena - Computers and Electrical Engineering, 2025 **Abstract:** The failure of the most potent medicines to eradicate superbugs underscores the urgent need to develop new antimicrobial drugs. Antibacterial peptides (ABPs) are oligopeptides present in all multicellular organisms and serve as the first line of defense against pathogens. ABPs provide several benefits over conventional antibiotics; therefore, they have recently gained significant attention as an alternative. Finding ABPs in the laboratory is expensive and time-consuming. Therefore, wet-lab researchers use *in-silico* tools to discover ABPs from natural sources. The existing tools available for this purpose suffer from the limitation of being black boxes. In the present work, we developed XAI-INVENT, an explainable artificial intelligence-based framework for the rapid discovery of novel antibiotics. For building XAI-INVENT, first, the probability scores of deep learning models are fused, and then the fused scores are utilized with local interpretable model-agnostic explanations (LIME) for determining the critical amino acids. The value of performance metrics, namely Accuracy, Sensitivity, Precision, F1-Score, Specificity, and Matthews correlation coefficient obtained by the proposed framework for test data is ≈ 96 %, 96 %, 97 %, 96 %, 97 %, and 92 %, respectively. To help wet-lab researchers, XAI-INVENT is deployed as a web server at https://xai-invent.anvil.app/.
79.	ZCLoRa: A lightweight deep learning based receiver for enhanced LoRa decoding **Irtizah, A Gupta, S Agarwal** - IEEE Communications Letters, 2025 **Abstract:** This letter introduces Zak-CNN LoRa (ZCLoRa), a novel receiver designed for low-power, long-range Internet of things (IoT) applications, addressing key limitations in conventional LoRa communication systems. In existing LoRa implementations, challenges such as low transmission power, unknown channel conditions, and degraded received signals lead to suboptimal decoding performance. To overcome these issues, we propose ZCLoRa, which leverages the Zak transform and exploits its sparse representation capabilities, enabling effective signal denoising. The Zak-transformed signal is processed by a convolutional neural network (CNN) for enhanced symbol decoding. We evaluate the performance of ZCLoRa in terms of symbol error rate (SER), showing significant improvements in decoding accuracy while maintaining the low complexity and power efficiency essential for IoT devices. Furthermore, we validate our model on USRPs, providing empirical evidence of its real-world effectiveness.

Disclaimer: This publication digest may not contain all the papers published. Library has compiled the publication data as per the alerts received from Scopus and Google Scholar for the affiliation "Indian Institute of Technology Ropar" for the month of **February, 2025**. The author(s) are requested to share their missing paper(s) details if any, for the inclusion in the next publication digest.